Blocking neutrophil integrin activation prevents ischemia–reperfusion injury

Tadayuki Yago,[1] Brian G. Petrich,[3,4] Nan Zhang,[2] Zhenghui Liu,[1] Bojing Shao,[1] Mark H. Ginsberg,[5] and Rodger P. McEver[1,2]

[1]Cardiovascular Biology Research Program, Oklahoma Medical Research Foundation, Oklahoma City, OK 73104
[2]Department of Biochemistry and Molecular Biology, University of Oklahoma Health Sciences Center, Oklahoma City, OK 73104
[3]Department of Pediatrics and [4]Aflac Cancer and Blood Disorders Center, Emory University School of Medicine, Atlanta, GA 30322
[5]Department of Medicine, University of California at San Diego, La Jolla, CA 92093

Neutrophil recruitment, mediated by β2 integrins, combats pyogenic infections but also plays a key role in ischemia–reperfusion injury and other inflammatory disorders. Talin induces allosteric rearrangements in integrins that increase affinity for ligands (activation). Talin also links integrins to actin and other proteins that enable formation of adhesions. Structural studies have identified a talin1 mutant (L325R) that perturbs activation without impairing talin's capacity to link integrins to actin and other proteins. Here, we found that mice engineered to express only talin1(L325R) in myeloid cells were protected from renal ischemia–reperfusion injury. Dissection of neutrophil function in vitro and in vivo revealed that talin1(L325R) neutrophils had markedly impaired chemokine-induced, β2 integrin–mediated arrest, spreading, and migration. Surprisingly, talin1(L325R) neutrophils exhibited normal selectin-induced, β2 integrin–mediated slow rolling, in sharp contrast to the defective slow rolling of neutrophils lacking talin1 or expressing a talin1 mutant (W359A) that blocks talin interaction with integrins. These studies reveal the importance of talin-mediated activation of integrins for renal ischemia–reperfusion injury. They further show that neutrophil arrest requires talin recruitment to and activation of integrins. However, although neutrophil slow rolling requires talin recruitment to integrins, talin-mediated integrin activation is dispensable.

CORRESPONDENCE
Rodger P. McEver:
rodger-mcever@omrf.org

Abbreviations used: ADAP, adhesion- and degranulation-promoting adaptor protein; ICAM-1, intercellular adhesion molecule-1; MD, membrane-distal; MP, membrane-proximal; PSGL-1, P-selectin glycoprotein ligand-1; PTx, pertussis toxin; SFK, Src family kinase; SLP-76, SH2-domain-containing leukocyte protein of 76 kD; Syk, spleen tyrosine kinase; TMD, transmembrane domain.

Rapid neutrophil recruitment is essential to combat pathogens (Nathan, 2006; Ley et al., 2007; Phillipson and Kubes, 2011). However, excessive neutrophil accumulation causes tissue injury in many inflammatory disorders, including ischemia–reperfusion of the kidney (Bonventre and Weinberg, 2003). In most organs, neutrophils roll along postcapillary venules, then arrest, spread, crawl to endothelial cell junctions, and migrate into perivascular tissues (Ley et al., 2007; Nourshargh et al., 2010). Endothelial cell selectins mediate rolling (McEver and Zhu, 2010). Neutrophil integrins, which are heterodimers composed of α and β subunits, enable arrest and crawling (Lefort and Ley, 2012). Signaling modulates neutrophil function (Zarbock et al., 2011). Neutrophils rolling on P-selectin engage P-selectin glycoprotein ligand-1 (PSGL-1), and neutrophils rolling on E-selectin engage PSGL-1 or CD44 (Zarbock et al., 2007; Yago et al., 2010b). These interactions trigger signals that convert the integrin αLβ2 ectodomain from a bent to an extended conformation, which retains a closed headpiece with low affinity for ligands (Kuwano et al., 2010). The extended, low-affinity integrin slows rolling by reversibly interacting with intercellular adhesion molecule-1 (ICAM-1) on activated endothelial cells. Notably, PSGL-1–triggered, αLβ2-mediated slow rolling requires neither intact actin filaments nor actomyosin-dependent tension (Shao et al., 2012). Slow rolling velocities enable neutrophil CXCR2 to interact with endothelial-bound chemokines such as CXCL1, which signal conversion of αLβ2 into an extended conformation with an open, high-affinity headpiece (Jung et al., 1998; Lefort and Ley, 2012). The extended,

The Rockefeller University Press $30.00
J. Exp. Med. 2015 Vol. 212 No. 8 1267–1281
www.jem.org/cgi/doi/10.1084/jem.20142358

The Journal of Experimental Medicine

high-affinity integrin mediates arrest on ICAM-1 and post-arrest outside-in signaling that strengthens adhesion and induces spreading (Yago et al., 2010b). Unlike slow rolling, arrest and spreading require actin filaments and actomyosin-dependent tension (Shao et al., 2012). Current evidence suggests that both selectin and chemokine signaling must be blocked to prevent neutrophil recruitment in many acute-inflammation models (Zarbock et al., 2007, 2008; Mueller et al., 2010; Yago et al., 2010b; Stadtmann et al., 2011). However, it was reported that blocking only selectin signaling prevents neutrophil-mediated injury to the kidney during ischemia and reperfusion (Block et al., 2012).

A final common step in integrin activation is binding of talin to the cytoplasmic domain (tail) of the β subunit (Kim et al., 2011; Ye et al., 2014). Talin is a large cytosolic protein with a head domain and a rod domain that interact with each other (Critchley, 2009). Cellular signals disrupt these intramolecular interactions and recruit talin to the membrane. The talin head domain binds to β tails, whereas the rod domain binds to β tails, actin, and other proteins. Talin1 is the predominant isoform expressed in hematopoietic cells. Talin1-deficient neutrophils cannot extend the αLβ2 ectodomain in response to selectin or chemokine signals (Lefort et al., 2012). They are defective in both αLβ2-mediated slow rolling and arrest on ICAM-1. Kindlins, another group of cytoplasmic adaptors, bind to a different region of the β tail (Moser et al., 2009b; Ye et al., 2014). Kindlin-3 is the predominate isoform expressed in hematopoietic cells. In response to selectin or chemokine signals, kindlin-3–deficient neutrophils extend the αLβ2 ectodomain but fail to open the headpiece (Lefort et al., 2012). Therefore, they exhibit αLβ2-dependent slow rolling but not arrest (Moser et al., 2009a; Lefort et al., 2012). These results, in conjunction with other studies (Bachir et al., 2014; Sun et al., 2014), suggest that kindlins facilitate talin-mediated integrin activation. Kindlins also increase the clustering of talin-activated integrins to augment adhesion strength (Ye et al., 2013), which in turn, stabilizes the open headpiece and promotes integrin outside-in signaling (Feigelson et al., 2011; Moretti et al., 2013; Xue et al., 2013).

Studies of platelet integrin αIIbβ3 have illuminated how talin binding to β tails initiates integrin activation. The talin head domain binds with high affinity to a membrane-distal (MD) motif on the β tail. This facilitates binding to a low-affinity, membrane-proximal (MP) site on the β tail (Vinogradova et al., 2002; Wegener et al., 2007). The MD and MP sequences are highly conserved in tails of β subunits. Talin binding to the MP region initiates integrin activation by two mechanisms. First, it weakens a juxtamembrane salt bridge between the α and β tails (Anthis et al., 2009; Saltel et al., 2009). Second, it stabilizes an α helix in the MP region to form a continuous α helix from the β transmembrane domain (TMD) into the MP region, and positions a basic patch in talin to bind to membrane phospholipids (Wegener et al., 2007; Anthis et al., 2009). This tripartite interaction increases the tilting angle of the β3 TMD, destabilizing αIIb-β3 TMD interactions that result in allosteric activation (Kim et al., 2012). A leucine residue (L325) in the talin head domain, located outside the interface with the rod domain (Song et al., 2012), forms a critical part of a hydrophobic region that interacts with two phenylalanines (F727 and F730 in β3) in the MP region (Wegener et al., 2007). A talin L325R mutation inhibits binding to the MP site but has little effect on the overall affinity of talin for the integrin. This mutation markedly reduces the ability of talin to increase tilting of the β3 TMD or to activate integrin αIIbβ3. Indeed, mice expressing only talin1(L325R) in their platelets exhibit a failure to activate integrin αIIbβ3 (Haling et al., 2011) and, as a result, manifest defective platelet aggregation, impaired platelet-mediated clot retraction, and severe bleeding (Haling et al., 2011; Stefanini et al., 2014). These in vitro and in vivo data provide strong evidence for the importance of talin binding to the MP region for allosteric activation of β3 integrins. However, separable functions of β3 integrins analogous to β2 integrin–mediated slow rolling and arrest have not been identified.

Here, we report the impact of the talin1 L325R mutation on neutrophil β2 integrin function in vitro and in vivo. Mice expressing talin1(L325R) only in myeloid cells were protected from renal ischemia–reperfusion injury, and their neutrophils failed to undergo chemokine-induced arrest, spreading, and migration. Unexpectedly, the neutrophils exhibited normal selectin-triggered, αLβ2-dependent slow rolling on ICAM-1. These data show that talin binding to the MP region of β2 tails is essential for neutrophil-mediated ischemia–reperfusion injury and for chemokine-triggered neutrophil arrest, but not for selectin-triggered slow rolling.

RESULTS

Mice expressing talin1(L325R) in neutrophils are protected from kidney ischemia–reperfusion injury

To determine whether talin1(L325R) can activate β2 integrins in neutrophils, we crossed *Tln1*$^{L325R/wt}$ mice, which express WT talin1 on one allele and talin1(L325R) on the other allele, with *Tln1*$^{f/f}$LysMCre^{+} mice, which make myeloid cells lacking *Tln1* on both alleles. *Tln1*$^{L325R/f}$LysMCre^{+} progeny make myeloid cells with one allele lacking *Tln1* and one allele expressing talin1(L325R). *Tln1*$^{wt/f}$LysMCre^{+} littermate controls make myeloid cells with one allele lacking *Tln1* and one allele expressing WT talin1. We used a similar strategy to generate *Tln1*$^{W359A/f}$LysMCre^{+} mice that make myeloid cells with one allele lacking *Tln1* and one allele expressing talin1(W359A). W359 in the talin1 head domain is located outside the interface with the rod domain (Song et al., 2012). A W359A mutation does not affect binding to the rod domain, but it markedly impairs binding to the high-affinity MD site on the integrin β3 tail (Wegener et al., 2007; Stefanini et al., 2014). We used heterozygous mice because global expression of talin1(L325R) or talin(W359A) on both alleles causes embryonic lethality (Haling et al., 2011), as observed in mice globally lacking talin1 (Monkley et al., 2000). Western blots with an antibody that recognizes both talin1 and talin2 confirmed deletion of talin1 and no detectable talin2 in neutrophils from *Tln1*$^{f/f}$LysMCre^{+}

mice compared with neutrophils from *Tln1*$^{f/f}$LysMCre^{-} control mice, which express WT talin1 on both alleles (Fig. 1 A). Neutrophils from *Tln1*$^{wt/f}$LysMCre^{+}, *Tln1*$^{L325R/f}$LysMCre^{+}, or *Tln1*$^{W359A/f}$LysMCre^{+} mice expressed ∼50% less talin, consistent with only one functional allele (Fig. 1 A). Quantitative PCR detected no mRNA for talin2 in bone marrow leukocytes of all genotypes, whereas mRNA for talin2 was readily detected in brain (unpublished data). Thus, deletion or mutation of talin1 in myeloid cells did not cause compensatory expression of talin2. Anti–β2 integrin antibody equivalently coprecipitated talin1 and talin1(L325R), but not talin1(W359A), from lysates of CXCL1-stimulated neutrophils (Fig. 1 B). This finding indicates that talin1(L325R), unlike talin1(W359A), retains its ability to bind to the MD site of the β2 integrin tail, as previously demonstrated for β3 integrins (Wegener et al., 2007; Haling et al., 2011; Stefanini et al., 2014). Mice of all genotypes were healthy and bred normally in the absence of challenge. Peripheral blood neutrophil counts were similarly elevated in *Tln1*$^{f/f}$LysMCre^{+} and *Tln1*$^{L325R/f}$LysMCre^{+} mice, but to a lesser degree than in *Itgb2*^{tm2Bay}/J (β2 integrin–deficient) mice (Table 1). Other blood counts were comparable in all genotypes (Table 1).

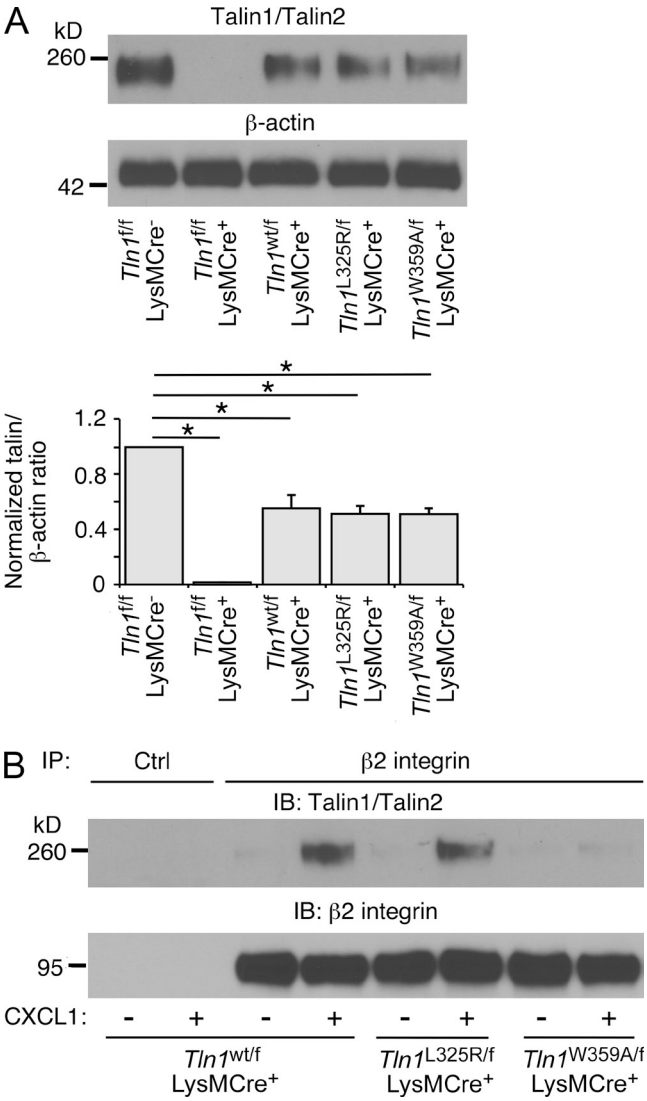

Figure 1. Murine neutrophils express equivalent levels of talin1, talin1(L325R), or talin1(W359A). (A, top) Representative Western blot of neutrophil lysates from the indicated genotype, probed with mAb 8d4, which recognizes both talin1 and talin2, or probed with rabbit anti–β-actin IgG. (bottom) Quantification of the talin/β-actin ratio by densitometry. (B) Neutrophils of the indicated genotype were incubated with or without CXCL1, lysed, and immunoprecipitated (IP) with control (Ctrl) or anti–β2 integrin mAb. Immunoprecipitates were analyzed by Western blotting (immunoblot, IB) with anti-talin and anti–β2 integrin antibodies. The data in A represent the mean ± SEM from three experiments. The data in B are representative of three experiments. *, $P < 0.01$, as determined by unpaired Student's *t* test.

Neutrophils contribute to kidney ischemia–reperfusion injury in mice (Singbartl et al., 2000; Singbartl and Ley, 2000; Bonventre and Weinberg, 2003; Li et al., 2010; Herter et al., 2014). We subjected mice to sham surgery or to surgery that included a 30-min clamp of both renal pedicles, followed by reperfusion for 24 h. In control mice, ischemia–reperfusion, but not sham surgery, markedly increased neutrophil infiltration and tubular necrosis in the kidneys (Fig. 2, A–D). Ischemia–reperfusion also elevated creatinine levels in plasma, indicating decreased glomerular filtration from tissue injury (Fig. 2 E). In contrast, ischemia–reperfusion did not induce neutrophil infiltration in *Tln1*$^{f/f}$LysMCre^{+} or *Tln1*$^{L325R/f}$LysMCre^{+} mice (Fig. 2, A and B). Furthermore, *Tln1*$^{f/f}$LysMCre^{+} and *Tln1*$^{L325R/f}$LysMCre^{+} mice exhibited significantly less tubular necrosis (Fig. 2, C and D) and elevation of plasma creatinine (Fig. 2 E), similar to that observed in neutrophil-depleted mice (Grenz et al., 2012). The neutrophil-independent component of acute kidney injury is primarily due to inadequate ATP production in epithelial cells during ischemia (Sharfuddin and Molitoris, 2011). We also observed markedly reduced neutrophil recruitment in kidneys of CXCR2-deficient (*Cxcr2*$^{-/-}$) mice, suggesting a major role for chemokine stimulation of neutrophils in this model (Fig. 2 A). These results demonstrate that blocking talin-mediated integrin activation in neutrophils by deleting talin1 or by the talin1(L325R) mutation reduces kidney ischemia–reperfusion injury.

Neutrophils expressing talin1(L325R) exhibit impaired entry into a site of inflammation

Selectins, chemokines, and β2 integrins promote neutrophil migration into the thioglycollate-challenged peritoneum (Robinson et al., 1999; Call et al., 2001; Smith et al., 2004), a classical model of acute inflammation. During the first 4 h after challenge, neutrophil recruitment is primarily dependent on integrin αLβ2 rather than αMβ2 (Coxon et al., 1996; Lu et al., 1997; Henderson et al., 2003). In control mice, we observed normal neutrophil migration into the peritoneum 4 h after thioglycollate injection, which was partially reduced by pretreating mice with pertussis toxin (PTx) to disable $G\alpha_i$-coupled chemokine receptors (Fig. 3 A). Migration was markedly decreased in both *Tln1*$^{f/f}$LysMCre^{+} and *Tln1*$^{L325R/f}$LysMCre^{+} mice, even without PTx pretreatment

Table 1. Peripheral blood counts

Genotype	WBC	NE	LY	MO	RBC	Hgb	PLT
	$\times 10^3/\mu l$	$\times 10^3/\mu l$	$\times 10^3/\mu l$	$\times 10^3/\mu l$	$\times 10^3/\mu l$	g/dl	$\times 10^3/\mu l$
WT (C57BL/6J) $n = 15$	4.6 ± 0.5	0.9 ± 0.1	3.6 ± 0.5	0.1 ± 0.0	10.1 ± 0.5	14 ± 1.5	1.0 ± 0.1
Itgb2^{tm2Bay}/J (C57BL/6J) $n = 5$	13.6 ± 1.0[a]	6.7 ± 1.0[a]	6.4 ± 1.0	0.3 ± 0.1	12.1 ± 0.5	12 ± 1.0	0.9 ± 0.1
Tln1$^{f/f}$LysMCre$^-$ $n = 7$	4.5 ± 0.5	1.0 ± 0.2	3.4 ± 0.5	0.1 ± 0.1	11.0 ± 1.0	11 ± 1.5	1.1 ± 0.1
Tln1$^{f/f}$LysMCre$^+$ $n = 7$	9.0 ± 1.0[b]	4.6 ± 1.0[b]	4.1 ± 1.0	0.3 ± 0.1	10.0 ± 0.5	12 ± 1.5	0.9 ± 0.1
Tln1$^{f/wt}$LysMCre$^+$ $n = 7$	5.1 ± 0.5	1.2 ± 0.3	3.8 ± 0.1	0.1 ± 0.0	9.8 ± 0.5	13 ± 1.5	1.1 ± 0.1
Tln1$^{f/L325R}$LysMCre$^+$ $n = 7$	8.3 ± 1.0[c]	4.0 ± 1.0[c]	4.0 ± 1.0	0.2 ± 0.0	10.5 ± 1.0	11 ± 1.0	0.9 ± 0.1

Hgb, hemoglobin; LY, lymphocytes; MO, monocytes; NE, neutrophils; PLT, platelets; RBC, red blood cells; WBC, white blood cells (total leukocytes). *Itgb2*^{tm2Bay}/J, β2 integrin–deficient mice in C57BL/6J background. The data represent the mean ± SEM.

[a]$P < 0.01$ vs. WT.

[b]$P < 0.01$ vs. *Tln1*$^{f/f}$LysMCre$^-$.

[c]$P < 0.01$ vs. *Tln1*$^{f/wt}$LysMCre$^+$.

(Fig. 3 A). To compare migration of neutrophils from different genotypes in the same mouse, we mixed control leukocytes labeled with a red dye with an equal number of control, *Tln1*$^{f/f}$LysMCre$^+$, or *Tln1*$^{L325R/f}$LysMCre$^+$ leukocytes labeled with a green dye. The cell mixture was injected intravenously into WT mice 2 h after injecting thioglycollate intraperitoneally. After another 2 h, a blood sample was obtained and peritoneal cells were collected. Neutrophils were counted for red and green fluorescence. Red and green cells in blood maintained a 1:1 ratio, confirming injection and survival of equal numbers of each population (Fig. 3 B). Mixtures of red and green control neutrophils entered the peritoneum in equal numbers. However, far fewer green *Tln1*$^{f/f}$LysMCre$^+$ or *Tln1*$^{L325R/f}$LysMCre$^+$ neutrophils entered the peritoneum than red control neutrophils (Fig. 3 B). These results demonstrate that blocking talin-mediated β2 integrin activation, by deleting talin1 or by the talin1(L325R) mutation, prevents neutrophil recruitment into the peritoneum after a potent inflammatory stimulus.

Neutrophils expressing talin1(L325R) manifest normal selectin-induced, β2 integrin–mediated slow rolling on ICAM-1 and defective chemokine-induced, β2 integrin–mediated arrest and spreading on ICAM-1

Murine bone marrow leukocytes roll on immobilized P- or E-selectin; >90% of the rolling cells are neutrophils. Selectin engagement induces integrin αLβ2-mediated slow rolling on coimmobilized ICAM-1. Coimmobilized CXCL1 induces αLβ2-mediated arrest and spreading on ICAM-1 (Miner et al., 2008; Yago et al., 2010b). Slow rolling and arrest are functional reporters of two distinct talin-mediated conformations of αLβ2. Selectin signals induce an extended conformation with a closed headpiece that retains low affinity for ICAM-1, whereas chemokine signals induce an extended conformation with an open, high-affinity headpiece (Kuwano et al., 2010). We confirmed published observations (Lefort et al., 2012) that talin1-deficient neutrophils from *Tln1*$^{f/f}$LysMCre$^+$ mice rolling on E-selectin (wall shear stress of 1 dyn/cm^2) failed to undergo either selectin-mediated slow rolling (Fig. 4 A) or CXCL1-mediated arrest on ICAM-1 (Fig. 4 D). Similar observations were made with neutrophils rolling on P-selectin (unpublished data). The arrest deficit was comparable to that of WT neutrophils treated with PTx to block $G\alpha_i$-coupled chemokine receptors (Fig. 4 G) or of CXCR2-deficient neutrophils (Fig. 4 H). Neutrophils from *Tln1*$^{W359A/f}$LysMCre$^+$ mice exhibited neither E-selectin–mediated slow rolling (Fig. 4 B) nor CXCL1-mediated arrest on ICAM-1 (Fig. 4 E), indicating that talin must bind to the MD site of the β2 tail for both slow rolling and arrest.

Based on the protection from kidney ischemia–reperfusion injury and the absence of thioglycollate-induced neutrophil recruitment, we predicted that neutrophils from *Tln1*$^{L325R/f}$LysMCre$^+$ mice would resist talin-mediated conformational change in response to selectin or chemokine signals. Indeed, neutrophils from *Tln1*$^{L325R/f}$LysMCre$^+$ mice rolling on E-selectin did not undergo CXCL1-mediated arrest and spreading on ICAM-1 (Fig. 4 F). Unexpectedly, however, they manifested normal E-selectin–mediated slow rolling on ICAM-1 (Fig. 4 C). Similar observations were made with neutrophils rolling on P-selectin (unpublished data). These data suggest that defective binding to the MP site on the β2 tail does not prevent integrin-associated talin1(L325R) from supporting slow rolling on ICAM-1.

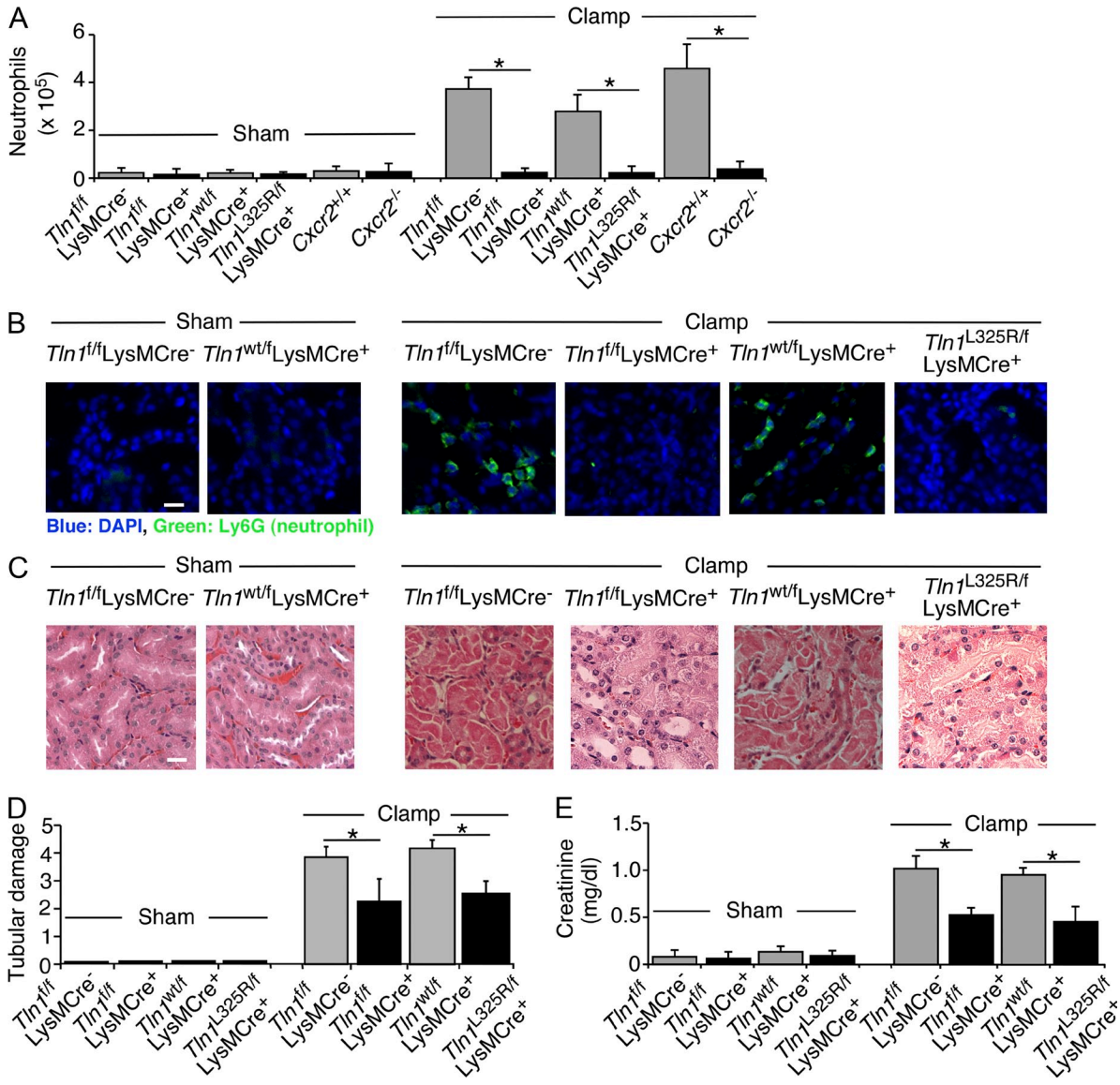

Figure 2. Mice expressing talin1(L325R) in neutrophils are protected from kidney ischemia–reperfusion injury. Mice of the indicated genotype were subjected to sham surgery or surgery that included a 30-min clamp of both renal pedicles to induce ischemia, followed by release of the clamp to permit reperfusion for 24 h. (A) Neutrophils infiltrating the kidneys were quantified by flow cytometry. (B) Immunofluorescence of representative kidney sections. Neutrophils were stained with anti-Ly6G mAb. Nuclei were counterstained with DAPI. Bar, 10 µm. (C) Representative kidney outer medulla sections stained with hematoxylin and eosin. Bar, 50 µm. (D) Tubular necrosis was quantified by epithelial karyolysis, necrotic debris, and cast formation as described in Materials and methods. (E) Creatinine levels in plasma. At least five mice were in each experimental group. The data in B and C are representative of five experiments. The data in A, D, and E represent the mean ± SEM from five experiments. *, $P < 0.01$, as determined by unpaired Student's *t* test.

To examine the contribution of talin1(L325R) to chemokine-induced β2 integrin activation independently of selectins, we incubated neutrophils under static conditions on control or ICAM-1–immobilized surfaces with or without coimmobilized CXCL1. Unbound neutrophils were then removed by perfusing cell-free buffer at low shear stress (0.25 dyn/cm^2). Control neutrophils, but not neutrophils lacking talin1 or expressing talin1(L325R), adhered specifically to ICAM-1 coimmobilized with CXCL1 (Fig. 4 I). Collectively, these results indicate that talin1(L325R) does not support chemokine-induced neutrophil adhesion to ICAM-1 under static or flow conditions, in the presence or absence of selectins.

Neutrophils expressing talin1(L325R) exhibit normal E-selectin–induced, β2 integrin–mediated slow rolling in venules

To determine whether talin1(L325R) can mediate β2 integrin–dependent slow rolling in vivo, we used intravital microscopy to visualize neutrophil rolling in venules of the cremaster muscle 4 h after intrascrotal injection of TNF, which induces endothelial expression of P- and E-selectin (Kunkel and Ley,

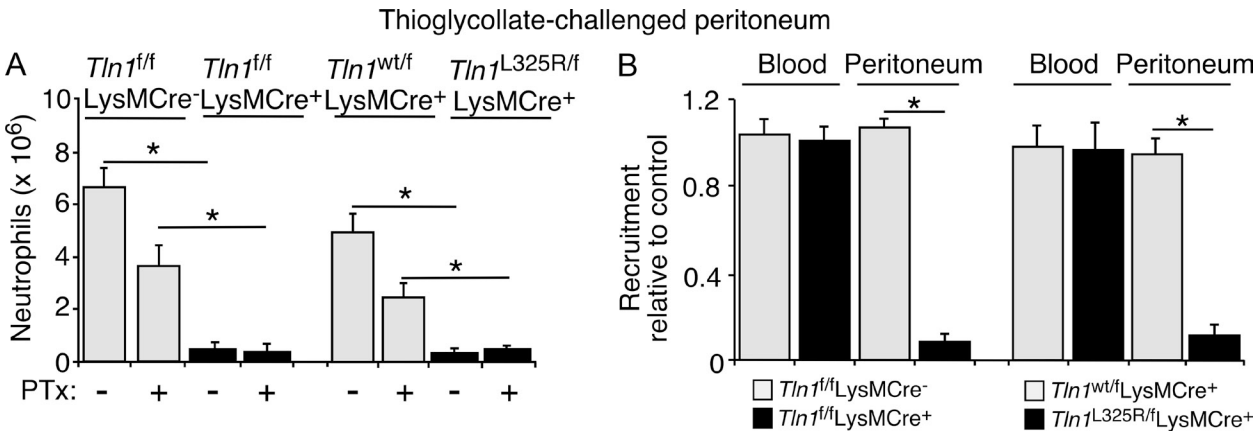

Figure 3. Neutrophils expressing talin1(L325R) exhibit impaired entry into a site of inflammation. (A) Untreated or PTx-pretreated mice of the indicated genotype were injected with thioglycollate intraperitoneally. After 4 h, peritoneal cells were collected, and the number of neutrophils was measured by flow cytometry. (B) Bone marrow leukocytes from control mice (*Tln1*$^{f/f}$LysMCre^{-} or *Tln1*$^{f/wt}$LysMCre^{+}) or experimental mice (*Tln1*$^{f/f}$LysMCre^{+} or *Tln1*$^{f/L325R}$LysMCre^{+}) were labeled with red (PKH26) or green (PKH67) dye. The labeled cells were resuspended at 10^8 cells/ml and mixed at a 1:1 ratio. Recipient mice were injected with thioglycollate intraperitoneally and, after 2 h, with 200 µl of the labeled cell mixture retroorbitally. After another 2 h, blood was collected. The mice were sacrificed, and peritoneal cells were collected. Neutrophils in blood and peritoneal exudate were counted. The data were plotted as the ratio of PKH26-labeled neutrophils from the experimental population compared with PKH67-labeled neutrophils from the control population. The data represent the mean ± SEM from five experiments, with at least five mice in each experimental group. *, $P < 0.01$ as determined by unpaired Student's *t* test.

1996). Hemodynamic and microvascular parameters in venules (Yago et al., 2010b) were equivalent in all genotypes (unpublished data). We injected PTx intravenously to block chemokine signaling through $G\alpha_i$-coupled receptors, and measured rolling velocities in the same venules before and after sequentially injecting blocking mAbs to P-selectin and β2 integrins. Anti–P-selectin mAb did not increase velocities, consistent with the dominance of E-selectin for rolling in this model (Kunkel and Ley, 1996). In control mice, Anti–β2 integrin mAb increased rolling velocities, confirming that slow rolling requires integrins (Fig. 5, A and B). As reported previously (Lefort et al., 2012), *Tln1*$^{f/f}$LysMCre^{+} neutrophils rolled faster than control neutrophils, and anti–β2 integrin mAb did not alter their velocities (Fig. 5 A). In sharp contrast, *Tln1*$^{L325R/f}$LysMCre^{+} neutrophils rolled slowly like control neutrophils, and their velocities increased after injecting anti–β2 integrin mAb (Fig. 5 B).

To directly compare rolling neutrophils from different genotypes in the same venules, we injected irradiated WT mice with WT LysM-GFP^{+} bone marrow cells mixed with an equal number of nonfluorescent bone marrow cells from each genotype. After reconstitution, we measured rolling velocities of fluorescent and nonfluorescent neutrophils in the same TNF-challenged venules in the cremaster muscle of mice pretreated with PTx and anti–P-selectin mAb. We confirmed loss of β2 integrin–dependent slow rolling in *Tln1*$^{f/f}$ LysMCre^{+} neutrophils (Fig. 5 C) but retention of slow rolling in *Tln1*$^{L325R/f}$LysMCre^{+} neutrophils (Fig. 5 D). These data demonstrate that talin1(L325R) mediates selectin-induced, β2 integrin–mediated slow rolling in vivo as well as in vitro.

To examine neutrophil rolling in the kidney, we labeled the membranes of control neutrophils with one fluorescent dye and the membranes of neutrophils lacking talin1 or expressing talin1(L325R) with another fluorescent dye. A 1:1 mixture of labeled control and mutant neutrophils was injected intravenously into WT mice subjected to kidney ischemia for 30 min, followed by reperfusion for 4 h. FITC-conjugated dextran was injected to visualize blood vessels. Spinning-disk confocal microscopy of the renal cortex was used to visualize rolling of labeled neutrophils in the same venules. Serial injection of blocking mAbs to P- and E-selectin detached all rolling cells (unpublished data). Injecting only anti–P-selectin mAb permitted specific study of E-selectin–mediated rolling and signaling (Fig. 5, E and F). Labeled *Tln1*$^{f/f}$LysMCre^{+} neutrophils rolled faster than control neutrophils in the same venules, and injection of anti–β2 integrin mAb did not alter their velocities (Fig. 5 E). In contrast, *Tln1*$^{L325R/f}$LysMCre^{+} neutrophils rolled slowly like control neutrophils in the same venules, and their velocities increased after injecting anti–β2 integrin mAb (Fig. 5 F). These data demonstrate that even when talin1-mediated slow rolling is intact, neutrophils require talin-mediated integrin activation to mediate kidney injury during ischemia–reperfusion.

Neutrophils expressing talin1(L325R) do not arrest in venules and do not emigrate out of venules

Intrascrotal injection of TNF increases expression of CXCL1 on venular surfaces in the cremaster muscle (Griffin et al., 2012; Yao et al., 2013). Endothelial CXCL1 activates integrin αLβ2 on slow-rolling neutrophils, inducing them to subsequently arrest and then emigrate out of venules in response to CXCL1 gradients (Phillipson et al., 2006; Massena et al., 2010; McDonald

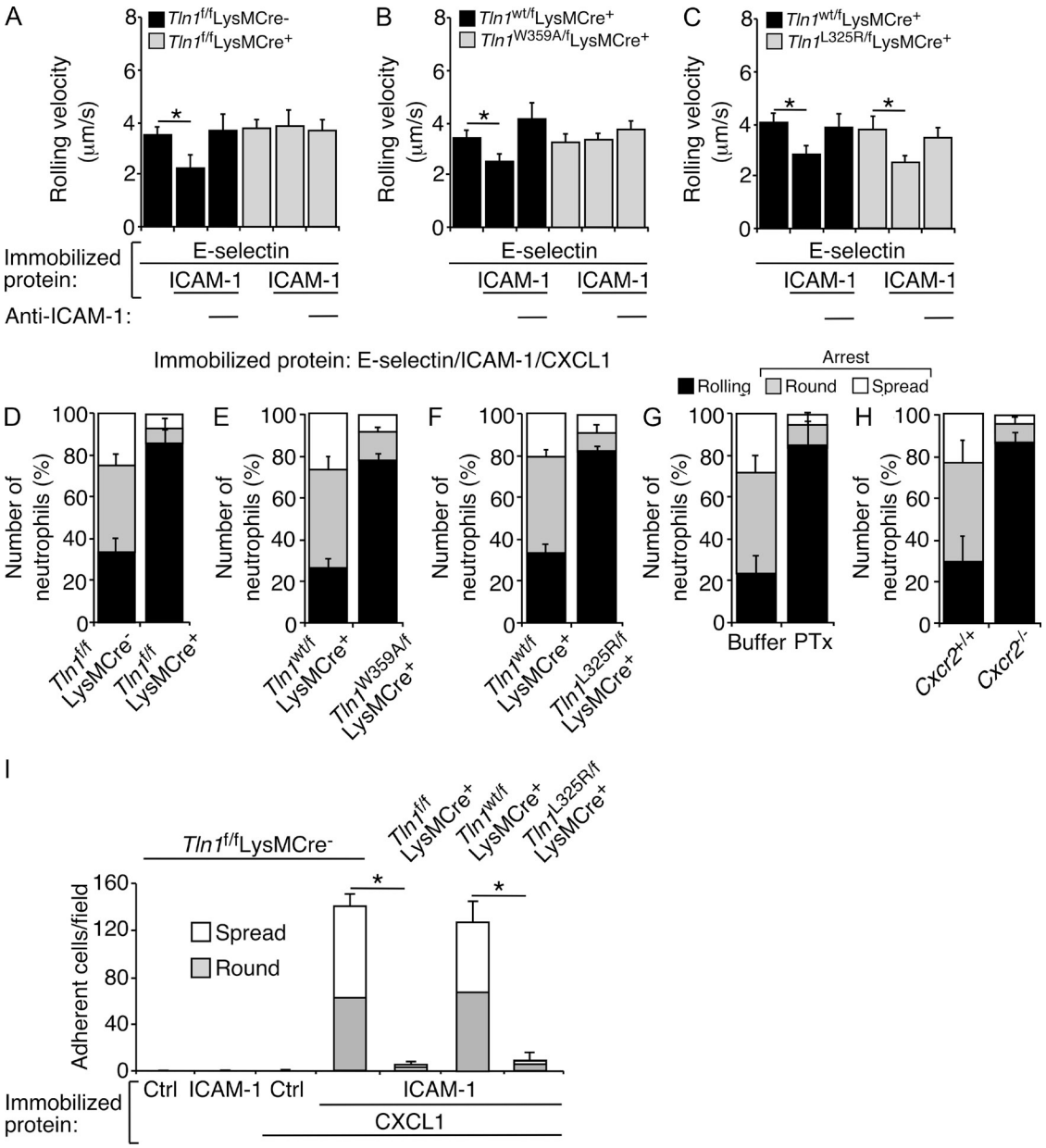

Figure 4. Neutrophils expressing talin1(L325R) manifest normal selectin-induced, β2 integrin–mediated slow rolling on ICAM-1 and defective chemokine-induced, β2 integrin–mediated arrest and spreading on ICAM-1. (A–C) Velocities of neutrophils of the indicated genotype rolling on E-selectin with or without coimmobilized ICAM-1 in the presence or absence of anti-ICAM-1 mAb. (D–H) Numbers of neutrophils of the indicated genotype rolling, arrested and round, or arrested and spread on coimmobilized E-selectin, ICAM-1, and CXCL1. The neutrophils in G were pretreated with PTx to block chemokine signaling through $G\alpha_i$-coupled receptors. The wall shear stress in A–H was 1 dyn/cm^2. (I) Numbers of neutrophils of the indicated genotype that adhered to control (Ctrl) or ICAM-1–immobilized surfaces with or without coimmobilized CXCL1 under static conditions. The data represent the mean ± SEM from five experiments, with at least five mice in each experimental group. *, $P < 0.01$, as determined by unpaired Student's *t* test.

et al., 2010). Current evidence suggests that both selectin signaling (to convert αLβ2 to an extended conformation with low affinity for ICAM-1) and chemokine signaling (to convert αLβ2 to an extended conformation with high affinity for ICAM-1) must be blocked to prevent neutrophil arrest and emigration (Zarbock et al., 2007, 2008; Mueller et al., 2010; Yago et al., 2010b; Stadtmann et al., 2011). We observed normal neutrophil arrest and emigration in control mice (Fig. 6, A and B). Pretreating mice with PTx to inhibit chemokine signaling reduced arrest and emigration by ∼50%, as noted previously (Yago et al., 2010b). In contrast, neutrophil arrest and emigration were markedly impaired in both *Tln1*$^{f/f}$LysMCre$^+$ and *Tln1*$^{L325R/f}$LysMCre$^+$ mice, even without PTx pretreatment (Fig. 6, A and B). These data establish that even when talin1-mediated slow rolling is intact, talin-mediated integrin activation is required to support neutrophil arrest and emigration in vivo.

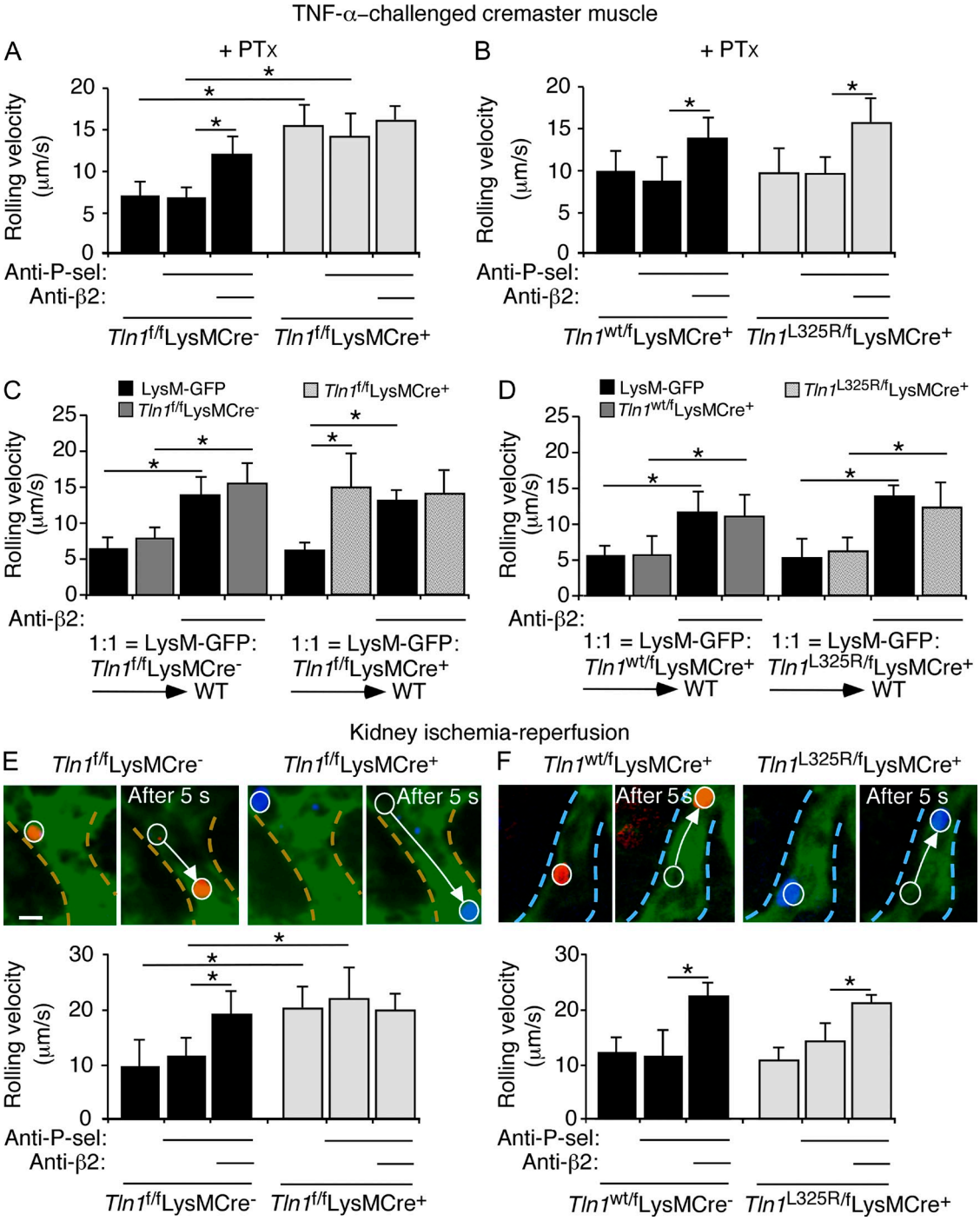

Figure 5. Neutrophils expressing talin1(L325R) exhibit normal E-selectin–induced, β2 integrin–mediated slow rolling in venules. (A and B) Velocities of neutrophils rolling in TNF-stimulated venules of cremaster muscle in mice of the indicated genotypes, measured before and after injecting a blocking mAb to P-selectin and then a blocking mAb to β2 integrins. The mice were pretreated with PTx to block chemokine signaling through $G\alpha_i$-coupled receptors. (C and D) Lethally irradiated WT mice were injected with WT LysM-GFP$^+$ bone marrow cells mixed with an equal number of GFP-negative cells of the indicated genotype. After eight weeks, the mice were treated with PTx and anti–P-selectin mAb, and rolling velocities of GFP-positive and GFP-negative neutrophils were measured in the same TNF-stimulated venules before and after injecting anti–β2 integrin mAb. (E and F) Velocities of differentially labeled bone marrow leukocytes from mice of the indicated genotype rolling in venules of the kidney cortex subjected to ischemia–reperfusion, before and after sequentially injecting blocking mAbs to P-selectin and β2 integrins. Representative fluorescent images (before injection of anti–β2 integrin mAb) illustrate distances rolled by control and mutant leukocytes over 5 s in the same venule visualized with FITC-dextran, outlined by the dashed line. The white arrow indicates the path of each rolling leukocyte. Bar, 10 μm. The data represent the mean ± SEM from five experiments, with at least five mice in each experimental group. *, $P < 0.01$ as determined by unpaired Student's *t* test.

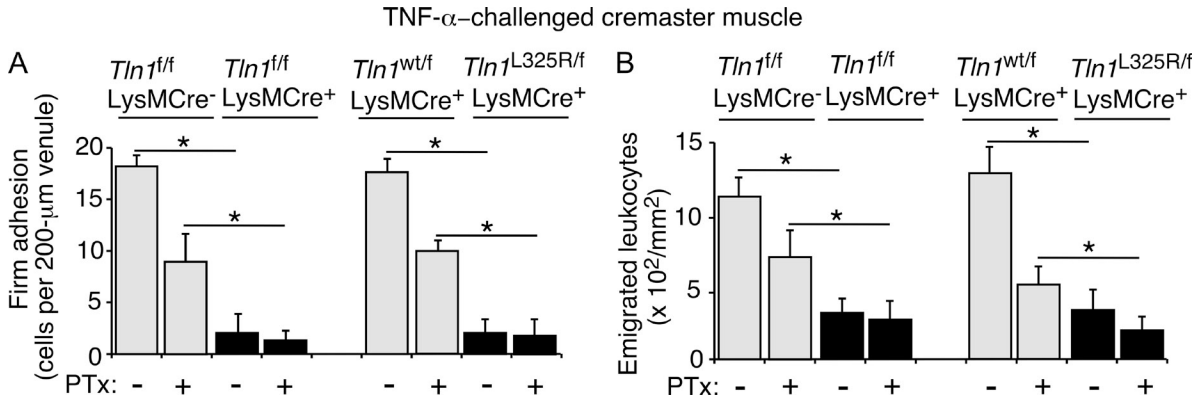

Figure 6. Neutrophils expressing talin1(L325R) do not arrest in venules and do not emigrate out of venules. (A) Numbers of firmly adherent neutrophils within venules and (B) numbers of emigrated neutrophils outside venules in TNF-stimulated cremaster muscle. As indicated, some mice were pretreated with PTx to block chemokine signaling through $G\alpha_i$-coupled receptors. The data represent the mean ± SEM from five experiments, with at least five mice in each experimental group. *, $P < 0.01$ as determined by unpaired Student's *t* test.

Talin1(L325R) strengthens adhesion when extracellular Mn^{2+} activates β2 integrins

Neutrophil adhesion to immobilized anti–β2 integrin mAb activates SFKs, spleen tyrosine kinase (Syk), Vav guanine nucleotide-exchange factors, and other mediators that rearrange the actin cytoskeleton and induce spreading (Gakidis et al., 2004; Mócsai et al., 2006; Abram and Lowell, 2009). Neutrophils lacking talin1 or expressing talin1(L325R) also spread normally on anti–β2 integrin mAb (Fig. 7, A and B). The Src family kinase (SFK) inhibitor PP2, but not its inactive analogue PP3, blocked spreading. Thus, β2 integrin outside-in signaling does not require talin, consistent with results obtained with other integrins (Arias-Salgado et al., 2005; Zhang et al., 2008).

Clot retraction supported by platelet integrin αIIbβ3 requires both talin1 (Haling et al., 2011) and outside-in signaling by SFKs and downstream components (Suzuki-Inoue et al., 2007). Talin1(L325R) supports clot retraction when integrin αIIbβ3 is activated by extracellular Mn^{2+}, because it retains the capacity to link integrins to the actin cytoskeleton (Haling et al., 2011). By analogy, we hypothesized that Mn^{2+} activation of β2 integrins would enable *Tln1*$^{L325R/f}$LysMCre$^+$ neutrophils to resist shear-induced detachment from ICAM-1. To test this hypothesis, we introduced leukocytes of different genotypes at low shear stress for 5 min into flow chambers coated with ICAM-1, which binds to integrins αLβ2 and αMβ2, or to fibrinogen, which binds to αMβ2. Mn^{2+} was added to the buffer to activate β2 integrins. We observed similar Mn^{2+}-dependent adhesion of *Tln1*$^{f/f}$LysMCre$^+$, *Tln1*$^{L325R/f}$LysMCre$^+$, or control neutrophils to ICAM-1 or fibrinogen (Fig. 7, C and E). To measure adhesion strength, we introduced cell-free buffer and measured adherent cells remaining after each step-wise increase in shear stress. *Tln1*$^{L325R/f}$LysMCre$^+$ neutrophils resisted detachment to the same extent as control cells. In sharp contrast, we observed greater shear-induced detachment of talin-deficient *Tln1*$^{f/f}$LysMCre$^+$ neutrophils (Fig. 7, D and F). These data demonstrate that β2 integrin–dependent adhesion strengthening requires talin-induced integrin activation. The activation requirement can be bypassed by exogenously activating integrins with Mn^{2+}. When talin is absent, however, Mn^{2+} activation is insufficient for adhesion strengthening, most likely because talin is also required to link integrins to the actin cytoskeleton.

DISCUSSION

Our results document an essential role for talin1-mediated activation of β2 integrins during renal ischemia–reperfusion injury. They also reveal separable talin effects on neutrophil β2 integrin function. Talin1-dependent neutrophil slow rolling is not sufficient for arrest on ICAM-1 or for subsequent neutrophil entry into an inflammatory site and resulting renal ischemia–reperfusion injury; the latter two events require talin-mediated integrin activation.

Tln1$^{L325R/f}$LysMCre$^+$ and control neutrophils mediated equivalent selectin-induced, β2 integrin–mediated slow rolling in vitro and in vivo (Figs. 4 and 5). This suggests similar conformations of αLβ2 in neutrophils of both genotypes. Reporter mAbs for human β2 integrins indicate that this conformation involves ectodomain extension without headpiece opening (Kuwano et al., 2010). Extending human αLβ2 while retaining a closed headpiece also permits transfected cells to roll on ICAM-1 (Salas et al., 2004). However, talin1 (L325R) might induce subtle rearrangements of the bent αLβ2 ectodomain that permit rapid binding to ICAM-1 without full extension.

The adhesive defects of *Tln1*$^{L325R/f}$LysMCre$^+$ neutrophils are similar but not identical to those of kindlin-3–deficient neutrophils (Lefort et al., 2012). Both exhibit selectin-induced, β2 integrin–mediated slow rolling but not chemokine-induced, β2 integrin–mediated arrest. Integrin outside-in signaling, measured as spreading on anti–integrin mAb or on physiological ligands when integrins are artificially activated, is defective in kindlin-3–deficient neutrophils or platelets (Moser et al., 2008; Moser et al., 2009a; Xue et al., 2013) but normal in

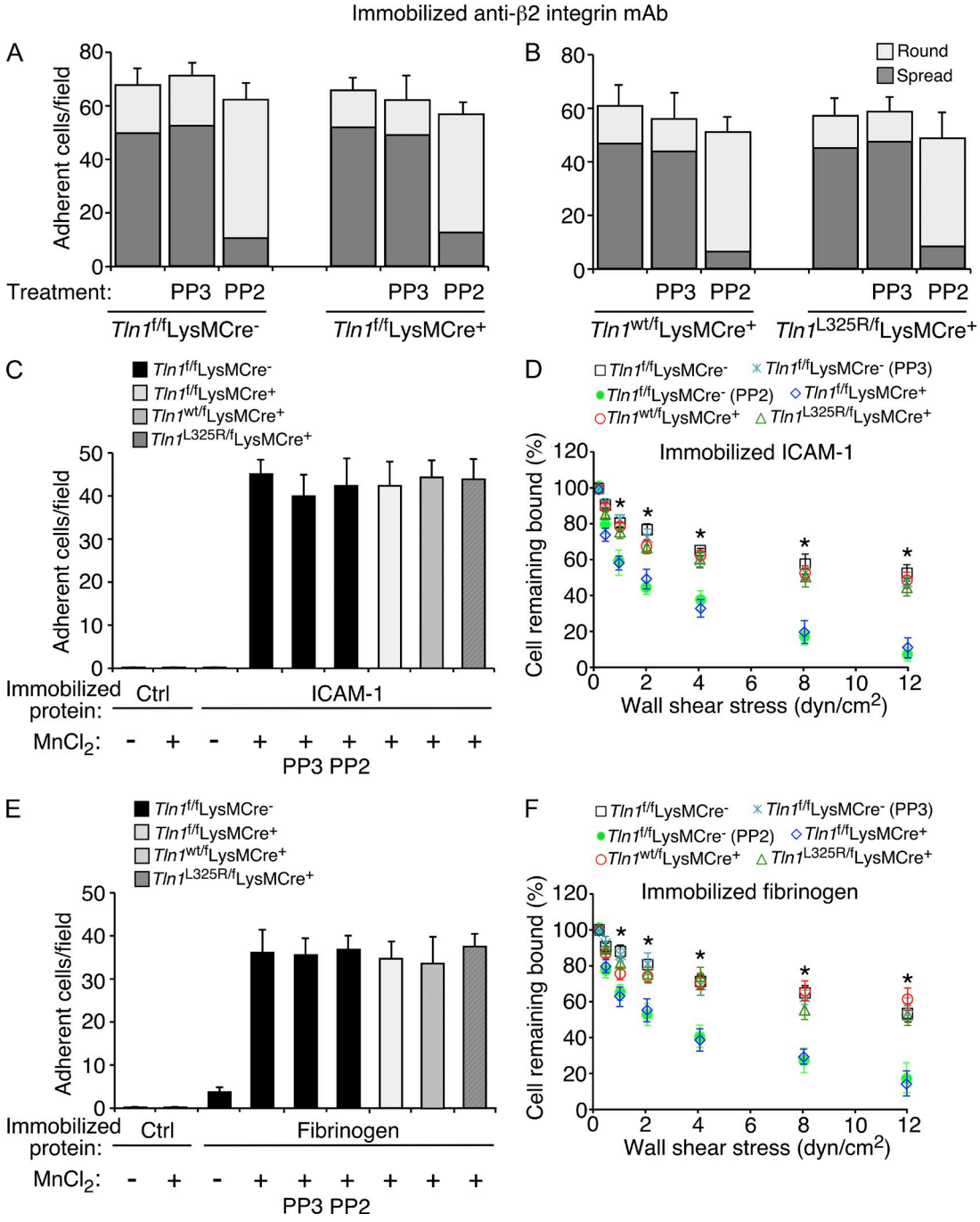

Figure 7. Talin1(L325R) strengthens adhesion when extracellular Mn^{2+}activates β2 integrins. (A and B) Numbers of neutrophils of the indicated genotype adherent and round or adherent and spread on immobilized anti–β2 integrin mAb. Neutrophils were pretreated with buffer only, the SFK inhibitor PP2, or the inactive analogue PP3. (C) Numbers of neutrophils of the indicated genotype adherent to a control (Ctrl) surface or to immobilized ICAM-1 at low wall shear stress (0.25 dyn/cm^2). As indicated, β2 integrins were activated with extracellular $MnCl_2$ or pretreated with PP3 or PP2. (D) Adhesion of $MnCl_2$-treated neutrophils of the indicated genotype at 0.25 dyn/cm^2 was measured as in panel C. The wall shear stress was then increased step-wise every 30 s, and the percentage of remaining adherent cells was determined. (E) Numbers of neutrophils of the indicated genotype adherent to a control (Ctrl) surface or to immobilized fibrinogen at low wall shear stress (0.25 dyn/cm^2). As indicated, β2 integrins were activated with extracellular $MnCl_2$ or pretreated with PP3 or PP2. (F) Adhesion of $MnCl_2$-treated neutrophils of the indicated genotype to fibrinogen at 0.25 dyn/cm^2 was measured as in E. The wall shear stress was then increased step-wise every 30 s, and the percentage of remaining adherent cells was determined. The data represent the mean ± SEM from five experiments, with at least five mice in each experimental group. *, $P < 0.01$ compared with *Tln1*$^{f/f}$LysMCre$^-$ (PP2) or *Tln1*$^{f/f}$LysMCre$^+$ neutrophils as determined by unpaired Student's *t* test.

talin1(L325R)-expressing neutrophils (Fig. 7 B). Talin1(L325R) supports platelet-mediated clot retraction when integrin αIIbβ3 is activated by extracellular Mn^{2+} (Haling et al., 2011). Similarly, *Tln1*$^{L325R/f}$LysMCre^{+} neutrophils exhibited normal SFK-dependent adhesion strengthening on fibrinogen or ICAM-1 when β2 integrins were activated by Mn^{2+} (Fig. 7, D and F). However, the inability of CXCL1 to trigger β2 integrin–dependent arrest prevented ligand-triggered outside-in signaling (Fig. 4 F), which for αIIbβ3, requires separation of the TMDs (Zhu et al., 2007). Kindlin-3–deficient leukocytes also have impaired adhesion strengthening (Feigelson et al., 2011; Moretti et al., 2013), probably from defects in both integrin clustering (Ye et al., 2013) and resulting outside-in signaling.

A W359A mutation inhibits talin1 binding to the MD site of the β3 tail and, as a result, hinders secondary binding to the MP site. In contrast, the L325R mutation impairs binding to the MP site without affecting the affinity for the MD site (Wegener et al., 2007). Neutrophils expressing talin1(W359A), like neutrophils lacking talin1, were deficient in both selectin-induced slow rolling and chemokine-induced arrest (Fig. 4, B and E), confirming that talin1 binding to the MD site of β tails is required to allosterically activate integrins (Tadokoro et al., 2003). The retention of selectin-induced slow rolling in neutrophils expressing talin1(L325R) supports the idea that binding to the MD site of the β tail permits talin to link integrins to cytoskeletal proteins such as actin and vinculin (Haling et al., 2011), although intact actin filaments are not required for slow rolling (Shao et al., 2012). The retention of slow rolling also suggests that shear forces applied to αLβ2-ICAM-1 bonds are sufficient for integrin extension (Chen et al., 2012). In static systems, the L325R mutation prevents the talin-induced tilting of the β3 transmembrane domain required for allosteric activation of αIIbβ3 (Wegener et al., 2007; Kim et al., 2012). Our finding that talin binding to the MP domain of the β subunit, which is blocked by the L325R mutation, is required for arrest indicates that the forces experienced during slow rolling are not sufficient to cause the headpiece opening associated with neutrophil arrest, even in the presence of chemokines. Thus, we propose that blocking talin's ability to engage the β2 integrin MP domain prevents the force-mediated cytoskeleton-dependent conversion of the ICAM-1–engaged chemokine-primed, closed headpiece, to the open headpiece, even when kindlin-3 is present (Chen et al., 2010; Schürpf and Springer, 2011; Alon and Feigelson, 2012; Shao et al., 2012).

We found that selectin-induced β2 integrin–mediated slow rolling is not sufficient for renal ischemia–reperfusion injury (Fig. 2) or for neutrophil emigration in response to other inflammatory stimuli (Figs. 3 and 6). Is selectin signaling necessary if not sufficient? For example, does selectin engagement prime neutrophils to respond more readily to chemokines? Previous studies concluded that selectin signaling cooperates with chemokine signaling to maximize neutrophil recruitment in models of acute inflammation (Zarbock et al., 2007, 2008; Mueller et al., 2010; Yago et al., 2010b; Stadtmann et al., 2011). However, these studies relied on inhibitors or gene knockouts that impair integrin-triggered outside-signals, as well as PSGL-1– or CD44-triggered inside-out signals. Both pathways share many features that canonical immunoreceptors use, including activation of SFKs and Syk and recruitment of SH2-domain–containing leukocyte protein of 76-kD (SLP-76), adhesion- and degranulation-promoting adaptor protein (ADAP), and other adaptors (Abram and Lowell, 2009; Zarbock et al., 2011). Mice with neutrophils lacking SLP-76 or ADAP are protected from renal ischemia–reperfusion injury, which was attributed solely to inhibiting selectin signaling (Block et al., 2012). However, renal protection in these mice probably resulted, at least in part, from inhibiting outside-in signaling by chemokine-activated integrins bound to ICAM-1 or other ligands. Defining the physiological relevance of selectin-triggered activation of β2 integrins will require methods to block signaling through selectin ligands, e.g., PSGL-1, without affecting integrin outside-in signaling. Mechanistic insights from such studies may reveal new targets for antiinflammatory drugs.

MATERIALS AND METHODS

Reagents. Murine P- and E-selectin IgM Fc chimeras and control murine CD45-IgM Fc chimera were described previously (Xia et al., 2002; Yago et al., 2010a). Murine ICAM-1 Fc, CXCL1, and TNF were purchased from R&D Systems. Rat anti–murine E-selectin mAb 9A9 and anti–murine P-selectin mAb RB40.34 have been previously described (Labow et al., 1994; Ley et al., 1995). The following mAbs to murine proteins were purchased from BD: rat anti-integrin αLβ2 (M17/4), rat anti-αMβ2 (M1/70), rat anti–β2 integrin (GAME-46), hamster anti–ICAM-1 (3E2), and biotinylated rat anti–murine Ly6G. Nonbiotinylated rat anti–murine Ly6G mAb was purchased from BioLegend. Murine mAb 8d4, which recognizes human and murine talin1 and talin2, murine fibrinogen, FITC-dextran (150 kD), and PKH26, PKH67, and CellVue Claret fluorescent dyes were purchased from Sigma-Aldrich. Rabbit polyclonal anti–β-actin IgG was purchased from Cell Signaling Technology. Rabbit polyclonal anti–β2 integrin antibody was purchased from Santa Cruz Biotechnology, Inc. Alexa Fluor 488–conjugated donkey anti–rat IgG antibody was purchased from Invitrogen. HRP-conjugated goat anti–murine IgG and goat anti–rabbit IgG were purchased from Thermo Fisher Scientific.

Mice. All mouse experiments were performed in compliance with protocols approved by the Institutional Animal Care and Use Committee of the Oklahoma Medical Research Foundation. C57BL/6J mice were purchased from The Jackson Laboratory. Mice lacking the integrin β2 subunit (*Itgb2*^{tm2Bay}/J) and mice lacking the chemokine receptor CXCR2 (*Cxcr2*^{Tm1Mwm}/J), both in the C57BL/6J background, were obtained from The Jackson Laboratory. LysM-GFP^{+} mice in the C57BL/6J background were described previously (Yao et al., 2013). Mice lacking talin1 in myeloid cells (*Tln1*$^{f/f}$LysMCre^{+}) were generated by breeding *Tln1*$^{f/f}$ mice (Petrich et al., 2007) with LysMCre^{+} mice in the C57BL/6J background (Yao et al., 2013). *Tln1*$^{f/f}$LysMCre^{-} mice were used as littermate controls for *Tln1*$^{f/f}$LysMCre^{+} mice. Mice expressing talin1(L325R) in myeloid cells (*Tln1*$^{L325R/f}$LysMCre^{+}) were generating by breeding *Tln1*$^{wt/L325R}$ mice (Haling et al., 2011) with *Tln1*$^{f/f}$LysMCre^{+} mice. Mice expressing talin1(W359A) in myeloid cells (*Tln1*$^{W359A/f}$LysMCre^{+}) were generating by breeding *Tln1*$^{wt/W359A}$ mice (Stefanini et al., 2014) with *Tln1*$^{f/f}$LysMCre^{+} mice. *Tln1*$^{wt/f}$LysMCre^{+} mice were used as littermate controls for *Tln1*$^{L325R/f}$LysMCre^{+} and *Tln1*$^{W359A/f}$LysMCre^{+} mice. All mice expressing *Tln1* genotypes were backcrossed into the C57BL/6J background for at least five generations. All mice were 8–12 wk old at time of study.

Renal ischemia–reperfusion injury. Renal ischemia–reperfusion injury was performed as previously described (Block et al., 2012). Mice were anesthetized by intraperitoneal injection of 1.25% Avertin. The mice were placed on a heating pad to maintain a constant temperature. A midline abdominal incision was made and then both kidneys were exposed. Renal ischemia was induced by nontraumatic vascular clamps of both pedicles for 30 min. After clamps were released, the incision was closed in two layers with 3–0 sutures. Sham-operated mice underwent the same procedure without clamping. After 24 h, the mice were euthanized. Blood samples were taken by heart puncture, and kidneys were harvested to evaluate neutrophil infiltration in the kidneys. Creatinine levels in plasma were measured with a kit (Arbor Assays). To determine the number of infiltrated neutrophils into the kidneys, single-cell suspensions were obtained by straining the collected kidneys through a 40-µm nylon mesh strainer. The suspension was labeled with PE-conjugated anti-Ly6G mAb for flow cytometric analysis. For histological analysis, the kidneys were fixed in 10% formalin, processed, and embedded in paraffin. Tissue sections were stained with hematoxylin and eosin. Tubular necrosis was evaluated by the percentage of tubules showing epithelial karyolysis, necrotic debris, or cast formation in 10–15 randomly selected sections at the corticomedullary junction and outer medulla from each group (Yamada et al., 2004). Tubular necrosis, examined at 40× magnification, was scored as follows: 0, none; 1+, <10%; 2+, 10–25%; 3+, 26–45%; 4+, 46–75%; 5+, >76%. The mean of the scores from the three morphological parameters in each group was used for statistical analysis. To assess neutrophil infiltration into the kidneys, kidneys were fixed in 4% paraformaldehyde overnight at 4°C, and then transferred into 20% sucrose overnight at 4°C for cryoprotection. Fixed tissues were mounted in OCT compound (Tissue-Tek 4583). After fixation in acetone at −20°C for 2 min, 5-µm cryosections were rinsed with PBS containing 0.01% saponin, incubated with Protein Block serum-free buffer (Dako) at room temperature for 60 min, and then incubated with rat anti–murine Ly6G mAb diluted in immunostain enhancer (Thermo Fisher Scientific) overnight at 4°C. The tissue sections were stained with Alexa Fluor 488–conjugated donkey anti–rat IgG antibody diluted in Protein Block buffer with 0.01% saponin at room temperature for 1 h. Mounting medium was then added to the slides. The images in the slides were visualized on an Axiovert 200M (Carl Zeiss) microscope at 63× magnification, and captured by a Carl Zeiss AxioCam MRm Rev. 3.0 camera using acquisition software AxioVision Ver. 4.8 (Carl Zeiss).

Thioglycollate-induced peritonitis. Neutrophil emigration into the thioglycollate-challenged peritoneum was performed as previously described (Yago et al., 2010b). Mice were injected intraperitoneally with 1 ml of 4% thioglycollate. Some mice received 4 µg PTx intravenously 2 h before thioglycollate injection. After 4 h, peritoneal cells were collected with 10 ml PBS containing 0.1% BSA and 5 mM EDTA, and the cells were analyzed by flow cytometry. Neutrophils were counted based on scatter properties and expression of Ly6G.

Competitive neutrophil recruitment assay. Competitive neutrophil recruitment was measured as previously described (Yago et al., 2010b). Bone marrow leukocytes from control mice (*Tln1*$^{f/f}$LysMCre^{-} or *Tln1*$^{f/wt}$LysMCre^{+}) or experimental mice (*Tln1*$^{f/f}$LysMCre^{+} or *Tln1*$^{f/L325R}$LysMCre^{+}) were labeled with red (PKH26) or green (PKH67) dye. The labeled cells were resuspended in HBSS at 10^8 cells/ml and mixed at a 1:1 ratio. Some labeled cells and recipient C57BL/6J mice were pretreated with PTx. Recipient mice were injected with 1 ml 4% thioglycollate intraperitoneally and, after 2 h, with 200 µl of the labeled cell mixture retroorbitally. After another 2 h, blood was collected. The mice were sacrificed, and peritoneal cells were collected with 10 ml PBS containing 0.1% BSA and 5 mM EDTA. Neutrophils in blood and peritoneal exudate were counted. The data were plotted as the ratio of PKH26-labeled neutrophils from the experimental population compared with PKH67-labeled neutrophils from the control population.

Bone marrow chimeras. Bone marrow chimeras were generated as described previously (Yao et al., 2013). In brief, bone marrow cells from LysM-GFP^{+} mice were mixed in a 1:1 ratio with bone marrow cells from *Tln1*$^{f/f}$LysMCre^{-}, *Tln1*$^{f/f}$LysMCre^{+}, *Tln1*$^{f/L325R}$LysMCre^{+}, or *Tln1*$^{f/wt}$LysMCre^{+} mice. The cells (4×10^6) were injected intravenously into lethally irradiated C57BL/6J mice. Intravital microscopy was performed 8 wk after bone marrow transplantation.

Flow chamber assay. Murine bone marrow leukocytes were isolated as described previously (Miner et al., 2008). In brief, bone marrow cells were isolated by gently flushing femurs and tibias with 10 ml Hanks' balanced salt solution (HBSS) without Ca^{2+} or Mg^{2+}. After lysing red blood cells in 150 mM NH_4Cl, 10 mM $NaHCO_3$, and 1 mM EDTA, the cells were washed with HBSS and resuspended at 2×10^6/ml in HBSS containing 1.26 mM Ca^{2+}, 0.81 mM Mg^{2+}, and 0.5% human serum albumin.

35-mm polystyrene dishes were adsorbed with 10 µg/ml goat anti–human IgM Fc antibody. In some experiments, 20 µg/ml murine ICAM-1–Fc and 10 µg/ml murine CXCL1 were also adsorbed. After incubation at 4°C overnight, the dishes were blocked with 1% human serum albumin, and then murine P-selectin or E-selectin–IgM was captured on the dishes. Bone marrow leukocytes were perfused over dishes mounted in a parallel-plate flow chamber at a wall shear stress of 1.0 dyn/cm^2. After 5–10 min, rolling and arrested cells were analyzed using a video microscopy system coupled to Element digital image-analysis software (Nikon). Arrested cells were scored as round (round and bright) or spread (irregular and dark). To block chemokine signaling through $G\alpha_i$-coupled receptors, some leukocytes were preincubated with 200 ng/ml PTx at 37°C for 2 h.

Alternatively, leukocytes were introduced into chambers containing dishes with or without immobilized ICAM-1 and/or CXCL1 at 0.25 dyn/cm^2 and then flow was stopped. After 15 min, unbound cells were removed with cell free-buffer at 0.25 dyn/cm^2, and then nonspread (round and bright) and spread (irregular and dark) cells were counted using Element software.

In some experiments, dishes were coated with 2 µg/ml ICAM-1 or 1 µg/ml fibrinogen and then blocked with 1% human serum albumin. Control surfaces were blocked with human serum albumin without adding ICAM-1 or fibrinogen. Neutrophils were isolated from bone marrow leukocytes by a density gradient method (Yao et al., 2013). The neutrophils were incubated with the SFK inhibitor PP2 (20 µM), its inactive analogue PP3 (20 µM), or 1 mM $MnCl_2$. They were introduced into chambers at 0.25 dyn/cm^2, and then flow was stopped. After 5 min, wall shear stress was increased step-wise every 30 s, and the number of remaining adherent cells was determined.

In other experiments, $F(ab')_2$ fragments of anti–murine β2 mAb GAME-46 were generated with a kit (Thermo Fisher Scientific). 50 µg/ml of GAME-46 $F(ab')_2$ were coated on 35-mm culture dishes. Neutrophils incubated with 20 µM PP2 or PP3 were introduced into the chamber at 0.25 dyn/cm^2 and then flow was stopped. After 15 min, unbound cells were removed with cell free-buffer at 0.25 dyn/cm^2, and then nonspread (round and bright) and spread (irregular and dark) cells were counted using Element software.

Immunoprecipitation and Western blot. Bone marrow leukocytes were incubated with Fc receptor blocker for 20 min at room temperature (Xia et al., 2002). They were then serially incubated (20 min at 4°C) with 10 µg/ml biotinylated rat anti-Ly6G mAb and with 5 µg/ml streptavidin-conjugated magnetic beads (Xia et al., 2004). Ly6G-positive neutrophils bound to magnetic beads were isolated on a magnetic separator (Xia et al., 2004). Flow cytometry confirmed that >99% of the isolated cells expressed Ly6G. Neutrophil lysates were probed by Western blotting as described previously (Yago et al., 2010b), using murine mAb 8d4, which recognizes both talin1 and talin2 (Zhang et al., 2008) or rabbit anti–β-actin IgG, followed by HRP-conjugated goat anti–mouse IgG or goat anti–rabbit IgG. The talin/β-actin ratio was quantified by densitometry.

In other experiments, neutrophils were isolated from bone marrow leukocytes by a density gradient (Yao et al., 2013). Cells (2×10^7) were incubated with or without 100 ng/ml CXCL1 for 10 min at 37°C, centrifuged, and lysed in 200 µl of 1% Triton X-100, 125 mM NaCl, 50 mM Tris, pH 7.4, 10 mM EDTA, 2 mM PMSF, 0.1% SDS with a protease inhibitor

cocktail (1:50; Thermo Fisher Scientific). Lysates were incubated with control rat IgG or rat anti–murine β2 integrin mAb GAME-46 and protein A/G agarose beads. After centrifugation, the beads were washed, and bound proteins were eluted by boiling in SDS-PAGE buffer with β-mercaptoethanol. The eluted proteins were probed by Western blotting with anti-talin mAb 8d4 or rabbit anti–β2 integrin antibody as described above.

Quantitative PCR. Total RNA from murine brains or bone marrow leukocytes was extracted with the RNeasy Plus Mini kit (QIAGEN). cDNA was prepared from 1.8 µg RNA in 20 µl H_2O using the High Capacity RNA-to-cDNA kit (Life Technologies). The levels of talin1 and talin2 cDNA were quantitated by quantitative PCR using IQ SYBR Green Supermix (Bio-Rad Laboratories) in 10-µl reactions under conditions of 1 cycle at 95°C for 10 min, and 40 cycles at 95°C for 15 s and 68°C for 1 min. Primers for murine talin1 were: 5′-CCGACTGGCCTCACAAGCCAAGCCT-3′ and 5′-GGCAGGTGGCTCTGGGGAACAGAAG-3′. Primers for murine talin2 were: 5′-GCACCTGGCTCTCCAGGGCCAGATG-3′ and 5′-TTCAGGTATGTCTTTTGACTGGAAC-3′. Standard curves for quantification of talin1 and talin2 were generated with purified plasmids encoding murine talin1 or talin2. Plasmids containing talin1 or talin2 genes were serially diluted in 10-fold steps, and quantified with quantitative PCR as above. The standard curves were plotted with the threshold cycle values against the concentrations of the purified plasmid (nanograms per microliter). The amounts of talin1 and talin2 cDNA prepared from 1 µg total RNA were calculated. GAPDH cDNA was used as internal control. Data from at least three independent sets were calculated as mean ± SD.

Intravital microscopy of cremaster muscle. Intravital microscopy was performed as described (Yao et al., 2013). In brief, mice were anesthetized by intraperitoneal injection of 1.25% Avertin (tribromoethanol/amylene hydrate, 0.2 ml/10 g body weight). The cremaster muscle was superfused with thermocontrolled (35°C) bicarbonate-buffer saline 3.5–4 h after intrascrotal injection of 500 ng murine TNF. In some experiments, mice received 4 µg PTx intravenously 2 h before cremaster muscle exteriorization. Mice were serially injected intravenously with blocking mAbs to P-selectin, E-selectin, or β2 integrins as indicated. Venule diameters, hemodynamic parameters, and mean leukocyte rolling fluxes and velocities were analyzed offline. The number of firmly adherent leukocytes within venules and the number of leukocytes emigrating outside venules were quantified.

Spinning-disk intravital microscopy of kidney. Spinning-disk intravital microscopy was performed to visualize real-time leukocyte adhesion to vessels in the kidney cortex. Mice were subjected to sham surgery or to 30 min of renal ischemia followed by reperfusion. After 4 h, the mice were reanesthetized, and the kidney was mobilized as described previously (Camirand et al., 2011). To minimize its motion, the kidney was moved onto a custom-made stage attached to supporting arms. A custom-made kidney holder with coverslip was placed on the kidney. The body temperature was maintained at 37°C by a heating pad coupled to a thermo-controller (Physitemp Instrument, Inc.). Bone marrow leukocytes from *Tln1*$^{f/f}$LysMCre^{-}, *Tln1*$^{f/f}$LysMCre^{+}, *Tln1*$^{f/L325R}$LysMCre^{+}, or *Tln1*$^{f/wt}$LysMCre^{+} mice were labeled with red fluorescent dye (PHK 26) or far-red fluorescent dye (CellVue Claret). The differentially labeled cells were resuspended in saline in a 1:1 mixture (10^8/ml), and 0.2 ml was injected intravenously. The vessels were labeled by intravenous injection of 100 µg FITC-dextran (150 kD)/mouse. In some experiments, 20 µg anti–P-selectin mAb and anti–E-selectin mAb were sequentially injected intravenously. In other experiments, 20 µg anti–P-selectin mAb and anti–β2 integrin mAb were sequentially injected intravenously. The microcirculation of the kidney cortex was observed using a Nikon ECLIPSE E600-FN upright microscope equipped with an Olympus 20×/0.95W XLUM Plan Fl water immersion objective lens. The microscope was coupled to a confocal light path (Solamere Technology Group) based on a modified Yokagawa CSU-X1 head (Yokagawa Electric Corporation). Three lasers with excitation at 488, 561, and 642 (Coherent) were rapidly and sequentially selected by an acousto-optic tunable filter, merged into a single optic cable, and introduced into the CSU-X1 head. Fluorescence signals were detected through three emission filters of ET525/50, ET605/52, and ET700/75 controlled by an ASI FW-1000 Filterwheel (Applied Scientific Instrumentation). A 512 × 512 pixel back-thinned EMCCD camera (C9100-13; Hamamatsu) was used for acquisition of the fluorescent images. The spinning disk confocal microscope was driven by the National Institutes of Health acquisition software Micromanager. The images were captured by Micromanager and analyzed with ImageJ software.

This work was supported by National Institutes of Health grants HL03463 to R.P. McEver, HL117061 to B.G. Petrich, and HL106489 to M.H. Ginsberg.

R.P. McEver has equity interest in Selexys Pharmaceuticals Corporation. The other authors declare no additional competing financial interests.

Submitted: 17 December 2014
Accepted: 9 June 2015

REFERENCES

Abram, C.L., and C.A. Lowell. 2009. The ins and outs of leukocyte integrin signaling. *Annu. Rev. Immunol.* 27:339–362. http://dx.doi.org/10.1146/annurev.immunol.021908.132554

Alon, R., and S.W. Feigelson. 2012. Chemokine-triggered leukocyte arrest: force-regulated bi-directional integrin activation in quantal adhesive contacts. *Curr. Opin. Cell Biol.* 24:670–676. http://dx.doi.org/10.1016/j.ceb.2012.06.001

Anthis, N.J., K.L. Wegener, F. Ye, C. Kim, B.T. Goult, E.D. Lowe, I. Vakonakis, N. Bate, D.R. Critchley, M.H. Ginsberg, and I.D. Campbell. 2009. The structure of an integrin/talin complex reveals the basis of inside-out signal transduction. *EMBO J.* 28:3623–3632. http://dx.doi.org/10.1038/emboj.2009.287

Arias-Salgado, E.G., S. Lizano, S.J. Shattil, and M.H. Ginsberg. 2005. Specification of the direction of adhesive signaling by the integrin beta cytoplasmic domain. *J. Biol. Chem.* 280:29699–29707. http://dx.doi.org/10.1074/jbc.M503508200

Bachir, A.I., J. Zareno, K. Moissoglu, E.F. Plow, E. Gratton, and A.R. Horwitz. 2014. Integrin-associated complexes form hierarchically with variable stoichiometry in nascent adhesions. *Curr. Biol.* 24:1845–1853. http://dx.doi.org/10.1016/j.cub.2014.07.011

Block, H., J.M. Herter, J. Rossaint, A. Stadtmann, S. Kliche, C.A. Lowell, and A. Zarbock. 2012. Crucial role of SLP-76 and ADAP for neutrophil recruitment in mouse kidney ischemia-reperfusion injury. *J. Exp. Med.* 209:407–421. http://dx.doi.org/10.1084/jem.20111493

Bonventre, J.V., and J.M. Weinberg. 2003. Recent advances in the pathophysiology of ischemic acute renal failure. *J. Am. Soc. Nephrol.* 14:2199–2210. http://dx.doi.org/10.1097/01.ASN.0000079785.13922.F6

Call, D.R., J.A. Nemzek, S.J. Ebong, G.L. Bolgos, D.E. Newcomb, and D.G. Remick. 2001. Ratio of local to systemic chemokine concentrations regulates neutrophil recruitment. *Am. J. Pathol.* 158:715–721. http://dx.doi.org/10.1016/S0002-9440(10)64014-X

Camirand, G., Q. Li, A.J. Demetris, S.C. Watkins, W.D. Shlomchik, D.M. Rothstein, and F.G. Lakkis. 2011. Multiphoton intravital microscopy of the transplanted mouse kidney. *Am. J. Transplant.* 11:2067–2074. http://dx.doi.org/10.1111/j.1600-6143.2011.03671.x

Chen, W., J. Lou, and C. Zhu. 2010. Forcing switch from short- to intermediate- and long-lived states of the alphaA domain generates LFA-1/ICAM-1 catch bonds. *J. Biol. Chem.* 285:35967–35978. http://dx.doi.org/10.1074/jbc.M110.155770

Chen, W., J. Lou, E.A. Evans, and C. Zhu. 2012. Observing force-regulated conformational changes and ligand dissociation from a single integrin on cells. *J. Cell Biol.* 199:497–512. http://dx.doi.org/10.1083/jcb.201201091

Coxon, A., P. Rieu, F.J. Barkalow, S. Askari, A.H. Sharpe, U.H. von Andrian, M.A. Arnaout, and T.N. Mayadas. 1996. A novel role for the beta 2 integrin CD11b/CD18 in neutrophil apoptosis: a homeostatic mechanism in inflammation. *Immunity.* 5:653–666. http://dx.doi.org/10.1016/S1074-7613(00)80278-2

Critchley, D.R. 2009. Biochemical and structural properties of the integrin-associated cytoskeletal protein talin. *Annu Rev Biophys*. 38:235–254. http://dx.doi.org/10.1146/annurev.biophys.050708.133744

Feigelson, S.W., V. Grabovsky, E. Manevich-Mendelson, R. Pasvolsky, Z. Shulman, V. Shinder, E. Klein, A. Etzioni, M. Aker, and R. Alon. 2011. Kindlin-3 is required for the stabilization of TCR-stimulated LFA-1: ICAM-1 bonds critical for lymphocyte arrest and spreading on dendritic cells. *Blood*. 117:7042–7052. http://dx.doi.org/10.1182/blood-2010-12-322859

Gakidis, M.A., X. Cullere, T. Olson, J.L. Wilsbacher, B. Zhang, S.L. Moores, K. Ley, W. Swat, T. Mayadas, and J.S. Brugge. 2004. Vav GEFs are required for beta2 integrin-dependent functions of neutrophils. *J. Cell Biol*. 166:273–282. http://dx.doi.org/10.1083/jcb.200404166

Grenz, A., J.H. Kim, J.D. Bauerle, E. Tak, H.K. Eltzschig, and E.T. Clambey. 2012. Adora2b adenosine receptor signaling protects during acute kidney injury via inhibition of neutrophil-dependent TNF-α release. *J. Immunol*. 189:4566–4573. http://dx.doi.org/10.4049/jimmunol.1201651

Griffin, G.K., G. Newton, M.L. Tarrio, D.X. Bu, E. Maganto-Garcia, V. Azcutia, P. Alcaide, N. Grabie, F.W. Luscinskas, K.J. Croce, and A.H. Lichtman. 2012. IL-17 and TNF-α sustain neutrophil recruitment during inflammation through synergistic effects on endothelial activation. *J. Immunol*. 188:6287–6299. http://dx.doi.org/10.4049/jimmunol.1200385

Haling, J.R., S.J. Monkley, D.R. Critchley, and B.G. Petrich. 2011. Talin-dependent integrin activation is required for fibrin clot retraction by platelets. *Blood*. 117:1719–1722. http://dx.doi.org/10.1182/blood-2010-09-305433

Henderson, R.B., J.A. Hobbs, M. Mathies, and N. Hogg. 2003. Rapid recruitment of inflammatory monocytes is independent of neutrophil migration. *Blood*. 102:328–335. http://dx.doi.org/10.1182/blood-2002-10-3228

Herter, J.M., J. Rossaint, T. Spieker, and A. Zarbock. 2014. Adhesion molecules involved in neutrophil recruitment during sepsis-induced acute kidney injury. *J. Innate Immun*. 6:597–606. http://dx.doi.org/10.1159/000358238

Jung, U., K.E. Norman, K. Scharffetter-Kochanek, A.L. Beaudet, and K. Ley. 1998. Transit time of leukocytes rolling through venules controls cytokine-induced inflammatory cell recruitment in vivo. *J. Clin. Invest*. 102:1526–1533. http://dx.doi.org/10.1172/JCI119893

Kim, C., F. Ye, and M.H. Ginsberg. 2011. Regulation of integrin activation. *Annu. Rev. Cell Dev. Biol*. 27:321–345. http://dx.doi.org/10.1146/annurev-cellbio-100109-104104

Kim, C., F. Ye, X. Hu, and M.H. Ginsberg. 2012. Talin activates integrins by altering the topology of the β transmembrane domain. *J. Cell Biol*. 197:605–611. http://dx.doi.org/10.1083/jcb.201112141

Kunkel, E.J., and K. Ley. 1996. Distinct phenotype of E-selectin-deficient mice. E-selectin is required for slow leukocyte rolling in vivo. *Circ. Res*. 79:1196–1204. http://dx.doi.org/10.1161/01.RES.79.6.1196

Kuwano, Y., O. Spelten, H. Zhang, K. Ley, and A. Zarbock. 2010. Rolling on E- or P-selectin induces the extended but not high-affinity conformation of LFA-1 in neutrophils. *Blood*. 116:617–624. http://dx.doi.org/10.1182/blood-2010-01-266122

Labow, M.A., C.R. Norton, J.M. Rumberger, K.M. Lombard-Gillooly, D.J. Shuster, J. Hubbard, R. Bertko, P.A. Knaack, R.W. Terry, M.L. Harbison, et al. 1994. Characterization of E-selectin-deficient mice: demonstration of overlapping function of the endothelial selectins. *Immunity*. 1:709–720. http://dx.doi.org/10.1016/1074-7613(94)90041-8

Lefort, C.T., and K. Ley. 2012. Neutrophil arrest by LFA-1 activation. *Front. Immunol*. 3:157. http://dx.doi.org/10.3389/fimmu.2012.00157

Lefort, C.T., J. Rossaint, M. Moser, B.G. Petrich, A. Zarbock, S.J. Monkley, D.R. Critchley, M.H. Ginsberg, R. Fässler, and K. Ley. 2012. Distinct roles for talin-1 and kindlin-3 in LFA-1 extension and affinity regulation. *Blood*. 119:4275–4282. http://dx.doi.org/10.1182/blood-2011-08-373118

Ley, K., D.C. Bullard, M.L. Arbonés, R. Bosse, D. Vestweber, T.F. Tedder, and A.L. Beaudet. 1995. Sequential contribution of L- and P-selectin to leukocyte rolling in vivo. *J. Exp. Med*. 181:669–675. http://dx.doi.org/10.1084/jem.181.2.669

Ley, K., C. Laudanna, M.I. Cybulsky, and S. Nourshargh. 2007. Getting to the site of inflammation: the leukocyte adhesion cascade updated. *Nat. Rev. Immunol*. 7:678–689. http://dx.doi.org/10.1038/nri2156

Li, L., L. Huang, A.L. Vergis, H. Ye, A. Bajwa, V. Narayan, R.M. Strieter, D.L. Rosin, and M.D. Okusa. 2010. IL-17 produced by neutrophils regulates IFN-gamma-mediated neutrophil migration in mouse kidney ischemia-reperfusion injury. *J. Clin. Invest*. 120:331–342. http://dx.doi.org/10.1172/JCI38702

Lu, H., C.W. Smith, J. Perrard, D. Bullard, L. Tang, S.B. Shappell, M.L. Entman, A.L. Beaudet, and C.M. Ballantyne. 1997. LFA-1 is sufficient in mediating neutrophil emigration in Mac-1-deficient mice. *J. Clin. Invest*. 99:1340–1350. http://dx.doi.org/10.1172/JCI119293

Massena, S., G. Christoffersson, E. Hjertström, E. Zcharia, I. Vlodavsky, N. Ausmees, C. Rolny, J.P. Li, and M. Phillipson. 2010. A chemotactic gradient sequestered on endothelial heparan sulfate induces directional intraluminal crawling of neutrophils. *Blood*. 116:1924–1931. http://dx.doi.org/10.1182/blood-2010-01-266072

McDonald, B., K. Pittman, G.B. Menezes, S.A. Hirota, I. Slaba, C.C. Waterhouse, P.L. Beck, D.A. Muruve, and P. Kubes. 2010. Intravascular danger signals guide neutrophils to sites of sterile inflammation. *Science*. 330:362–366. http://dx.doi.org/10.1126/science.1195491

McEver, R.P., and C. Zhu. 2010. Rolling cell adhesion. *Annu. Rev. Cell Dev. Biol*. 26:363–396. http://dx.doi.org/10.1146/annurev.cellbio.042308.113238

Miner, J.J., L. Xia, T. Yago, J. Kappelmayer, Z. Liu, A.G. Klopocki, B. Shao, J.M. McDaniel, H. Setiadi, D.W. Schmidtke, and R.P. McEver. 2008. Separable requirements for cytoplasmic domain of PSGL-1 in leukocyte rolling and signaling under flow. *Blood*. 112:2035–2045. http://dx.doi.org/10.1182/blood-2008-04-149468

Mócsai, A., C.L. Abram, Z. Jakus, Y. Hu, L.L. Lanier, and C.A. Lowell. 2006. Integrin signaling in neutrophils and macrophages uses adaptors containing immunoreceptor tyrosine-based activation motifs. *Nat. Immunol*. 7:1326–1333. http://dx.doi.org/10.1038/ni1407

Monkley, S.J., X.H. Zhou, S.J. Kinston, S.M. Giblett, L. Hemmings, H. Priddle, J.E. Brown, C.A. Pritchard, D.R. Critchley, and R. Fässler. 2000. Disruption of the talin gene arrests mouse development at the gastrulation stage. *Dev. Dyn*. 219:560–574. http://dx.doi.org/10.1002/1097-0177(2000)9999:9999<::AID-DVDY1079>3.0.CO;2-Y

Moretti, F.A., M. Moser, R. Lyck, M. Abadier, R. Ruppert, B. Engelhardt, and R. Fässler. 2013. Kindlin-3 regulates integrin activation and adhesion reinforcement of effector T cells. *Proc. Natl. Acad. Sci. USA*. 110:17005–17010. http://dx.doi.org/10.1073/pnas.1316032110

Moser, M., B. Nieswandt, S. Ussar, M. Pozgajova, and R. Fässler. 2008. Kindlin-3 is essential for integrin activation and platelet aggregation. *Nat. Med*. 14:325–330. http://dx.doi.org/10.1038/nm1722

Moser, M., M. Bauer, S. Schmid, R. Ruppert, S. Schmidt, M. Sixt, H.-V. Wang, M. Sperandio, and R. Fässler. 2009a. Kindlin-3 is required for beta2 integrin-mediated leukocyte adhesion to endothelial cells. *Nat. Med*. 15:300–305. http://dx.doi.org/10.1038/nm.1921

Moser, M., K.R. Legate, R. Zent, and R. Fässler. 2009b. The tail of integrins, talin, and kindlins. *Science*. 324:895–899. http://dx.doi.org/10.1126/science.1163865

Mueller, H., A. Stadtmann, H. Van Aken, E. Hirsch, D. Wang, K. Ley, and A. Zarbock. 2010. Tyrosine kinase Btk regulates E-selectin–mediated integrin activation and neutrophil recruitment by controlling phospholipase C (PLC) gamma2 and PI3Kgamma pathways. *Blood*. 115:3118–3127. http://dx.doi.org/10.1182/blood-2009-11-254185

Nathan, C. 2006. Neutrophils and immunity: challenges and opportunities. *Nat. Rev. Immunol*. 6:173–182. http://dx.doi.org/10.1038/nri1785

Nourshargh, S., P.L. Hordijk, and M. Sixt. 2010. Breaching multiple barriers: leukocyte motility through venular walls and the interstitium. *Nat. Rev. Mol. Cell Biol*. 11:366–378. http://dx.doi.org/10.1038/nrm2889

Petrich, B.G., P. Marchese, Z.M. Ruggeri, S. Spiess, R.A. Weichert, F. Ye, R. Tiedt, R.C. Skoda, S.J. Monkley, D.R. Critchley, and M.H. Ginsberg. 2007. Talin is required for integrin-mediated platelet function in hemostasis and thrombosis. *J. Exp. Med*. 204:3103–3111. http://dx.doi.org/10.1084/jem.20071800

Phillipson, M., and P. Kubes. 2011. The neutrophil in vascular inflammation. *Nat. Med*. 17:1381–1390. http://dx.doi.org/10.1038/nm.2514

Phillipson, M., B. Heit, P. Colarusso, L. Liu, C.M. Ballantyne, and P. Kubes. 2006. Intraluminal crawling of neutrophils to emigration sites: a molecularly distinct process from adhesion in the recruitment cascade. *J. Exp. Med*. 203:2569–2575. http://dx.doi.org/10.1084/jem.20060925

Robinson, S.D., P.S. Frenette, H. Rayburn, M. Cummiskey, M. Ullman-Culleré, D.D. Wagner, and R.O. Hynes. 1999. Multiple, targeted deficiencies in selectins reveal a predominant role for P-selectin in leukocyte recruitment. *Proc. Natl. Acad. Sci. USA*. 96:11452–11457. http://dx.doi.org/10.1073/pnas.96.20.11452

Salas, A., M. Shimaoka, A.N. Kogan, C. Harwood, U.H. von Andrian, and T.A. Springer. 2004. Rolling adhesion through an extended conformation of integrin alphaLbeta2 and relation to alpha I and beta I-like domain interaction. *Immunity*. 20:393–406. http://dx.doi.org/10.1016/S1074-7613(04)00082-2

Saltel, F., E. Mortier, V.P. Hytönen, M.C. Jacquier, P. Zimmermann, V. Vogel, W. Liu, and B. Wehrle-Haller. 2009. New PI(4,5)P2- and membrane proximal integrin-binding motifs in the talin head control beta3-integrin clustering. *J. Cell Biol.* 187:715–731. http://dx.doi.org/10.1083/jcb.200908134

Schürpf, T., and T.A. Springer. 2011. Regulation of integrin affinity on cell surfaces. *EMBO J.* 30:4712–4727. http://dx.doi.org/10.1038/emboj.2011.333

Shao, B., T. Yago, P.A. Coghill, A.G. Klopocki, P. Mehta-D'souza, D.W. Schmidtke, W. Rodgers, and R.P. McEver. 2012. Signal-dependent slow leukocyte rolling does not require cytoskeletal anchorage of P-selectin glycoprotein ligand-1 (PSGL-1) or integrin αLβ2. *J. Biol. Chem.* 287:19585–19598. http://dx.doi.org/10.1074/jbc.M112.361519

Sharfuddin, A.A., and B.A. Molitoris. 2011. Pathophysiology of ischemic acute kidney injury. *Nat. Rev. Nephrol.* 7:189–200. http://dx.doi.org/10.1038/nrneph.2011.16

Singbartl, K., and K. Ley. 2000. Protection from ischemia-reperfusion induced severe acute renal failure by blocking E-selectin. *Crit. Care Med.* 28:2507–2514. http://dx.doi.org/10.1097/00003246-200007000-00053

Singbartl, K., S.A. Green, and K. Ley. 2000. Blocking P-selectin protects from ischemia/reperfusion-induced acute renal failure. *FASEB J.* 14:48–54.

Smith, M.L., T.S. Olson, and K. Ley. 2004. CXCR2- and E-selectin–induced neutrophil arrest during inflammation in vivo. *J. Exp. Med.* 200:935–939. http://dx.doi.org/10.1084/jem.20040424

Song, X., J. Yang, J. Hirbawi, S. Ye, H.D. Perera, E. Goksoy, P. Dwivedi, E.F. Plow, R. Zhang, and J. Qin. 2012. A novel membrane-dependent on/off switch mechanism of talin FERM domain at sites of cell adhesion. *Cell Res.* 22:1533–1545. http://dx.doi.org/10.1038/cr.2012.97

Stadtmann, A., L. Brinkhaus, H. Mueller, J. Rossaint, M. Bolomini-Vittori, W. Bergmeier, H. Van Aken, D.D. Wagner, C. Laudanna, K. Ley, and A. Zarbock. 2011. Rap1a activation by CalDAG-GEFI and p38 MAPK is involved in E-selectin-dependent slow leukocyte rolling. *Eur. J. Immunol.* 41:2074–2085. http://dx.doi.org/10.1002/eji.201041196

Stefanini, L., F. Ye, A.K. Snider, K. Sarabakhsh, R. Piatt, D.S. Paul, W. Bergmeier, and B.G. Petrich. 2014. A talin mutant that impairs talin-integrin binding in platelets decelerates αIIbβ3 activation without pathological bleeding. *Blood*. 123:2722–2731. http://dx.doi.org/10.1182/blood-2013-12-543363

Sun, H., J. Liu, Y. Zheng, Y. Pan, K. Zhang, and J. Chen. 2014. Distinct chemokine signaling regulates integrin ligand specificity to dictate tissue-specific lymphocyte homing. *Dev. Cell.* 30:61–70. http://dx.doi.org/10.1016/j.devcel.2014.05.002

Suzuki-Inoue, K., C.E. Hughes, O. Inoue, M. Kaneko, O. Cuyun-Lira, T. Takafuta, S.P. Watson, and Y. Ozaki. 2007. Involvement of Src kinases and PLCgamma2 in clot retraction. *Thromb. Res.* 120:251–258. http://dx.doi.org/10.1016/j.thromres.2006.09.003

Tadokoro, S., S.J. Shattil, K. Eto, V. Tai, R.C. Liddington, J.M. de Pereda, M.H. Ginsberg, and D.A. Calderwood. 2003. Talin binding to integrin beta tails: a final common step in integrin activation. *Science*. 302:103–106. http://dx.doi.org/10.1126/science.1086652

Vinogradova, O., A. Velyvis, A. Velyviene, B. Hu, T. Haas, E. Plow, and J. Qin. 2002. A structural mechanism of integrin alpha(IIb)beta(3) "inside-out" activation as regulated by its cytoplasmic face. *Cell.* 110:587–597. http://dx.doi.org/10.1016/S0092-8674(02)00906-6

Wegener, K.L., A.W. Partridge, J. Han, A.R. Pickford, R.C. Liddington, M.H. Ginsberg, and I.D. Campbell. 2007. Structural basis of integrin activation by talin. *Cell.* 128:171–182. http://dx.doi.org/10.1016/j.cell.2006.10.048

Xia, L., M. Sperandio, T. Yago, J.M. McDaniel, R.D. Cummings, S. Pearson-White, K. Ley, and R.P. McEver. 2002. P-selectin glycoprotein ligand-1-deficient mice have impaired leukocyte tethering to E-selectin under flow. *J. Clin. Invest.* 109:939–950. http://dx.doi.org/10.1172/JCI0214151

Xia, L., J.M. McDaniel, T. Yago, A. Doeden, and R.P. McEver. 2004. Surface fucosylation of human cord blood cells augments binding to P-selectin and E-selectin and enhances engraftment in bone marrow. *Blood*. 104:3091–3096. http://dx.doi.org/10.1182/blood-2004-02-0650

Xue, Z.H., C. Feng, W.L. Liu, and S.M. Tan. 2013. A role of kindlin-3 in integrin αMβ2 outside-in signaling and the Syk-Vav1-Rac1/Cdc42 signaling axis. *PLoS ONE*. 8:e56911. http://dx.doi.org/10.1371/journal.pone.0056911

Yago, T., J. Fu, J.M. McDaniel, J.J. Miner, R.P. McEver, and L. Xia. 2010a. Core 1-derived O-glycans are essential E-selectin ligands on neutrophils. *Proc. Natl. Acad. Sci. USA*. 107:9204–9209. http://dx.doi.org/10.1073/pnas.1003110107

Yago, T., B. Shao, J.J. Miner, L. Yao, A.G. Klopocki, K. Maeda, K.M. Coggeshall, and R.P. McEver. 2010b. E-selectin engages PSGL-1 and CD44 through a common signaling pathway to induce integrin alphaLbeta2–mediated slow leukocyte rolling. *Blood*. 116:485–494. http://dx.doi.org/10.1182/blood-2009-12-259556

Yamada, K., T. Miwa, J. Liu, M. Nangaku, and W.C. Song. 2004. Critical protection from renal ischemia reperfusion injury by CD55 and CD59. *J. Immunol.* 172:3869–3875. http://dx.doi.org/10.4049/jimmunol.172.6.3869

Yao, L., T. Yago, B. Shao, Z. Liu, R. Silasi-Mansat, H. Setiadi, F. Lupu, and R.P. McEver. 2013. Elevated CXCL1 expression in gp130-deficient endothelial cells impairs neutrophil migration in mice. *Blood*. 122:3832–3842. http://dx.doi.org/10.1182/blood-2012-12-473835

Ye, F., B.G. Petrich, P. Anekal, C.T. Lefort, A. Kasirer-Friede, S.J. Shattil, R. Ruppert, M. Moser, R. Fässler, and M.H. Ginsberg. 2013. The mechanism of kindlin-mediated activation of integrin αIIbβ3. *Curr. Biol.* 23:2288–2295. http://dx.doi.org/10.1016/j.cub.2013.09.050

Ye, F., A.K. Snider, and M.H. Ginsberg. 2014. Talin and kindlin: the one-two punch in integrin activation. *Fr. Medecine*. 8:6–16. http://dx.doi.org/10.1007/s11684-014-0317-3

Zarbock, A., C.A. Lowell, and K. Ley. 2007. Spleen tyrosine kinase Syk is necessary for E-selectin–induced $\alpha_{(L)}\beta_{(2)}$ integrin-mediated rolling on intercellular adhesion molecule-1. *Immunity*. 26:773–783. http://dx.doi.org/10.1016/j.immuni.2007.04.011

Zarbock, A., C.L. Abram, M. Hundt, A. Altman, C.A. Lowell, and K. Ley. 2008. PSGL-1 engagement by E-selectin signals through Src kinase Fgr and ITAM adapters DAP12 and FcR gamma to induce slow leukocyte rolling. *J. Exp. Med.* 205:2339–2347. http://dx.doi.org/10.1084/jem.20072660

Zarbock, A., K. Ley, R.P. McEver, and A. Hidalgo. 2011. Leukocyte ligands for endothelial selectins: specialized glycoconjugates that mediate rolling and signaling under flow. *Blood*. 118:6743–6751. http://dx.doi.org/10.1182/blood-2011-07-343566

Zhang, X., G. Jiang, Y. Cai, S.J. Monkley, D.R. Critchley, and M.P. Sheetz. 2008. Talin depletion reveals independence of initial cell spreading from integrin activation and traction. *Nat. Cell Biol.* 10:1062–1068. http://dx.doi.org/10.1038/ncb1765

Zhu, J., C.V. Carman, M. Kim, M. Shimaoka, T.A. Springer, and B.H. Luo. 2007. Requirement of alpha and beta subunit transmembrane helix separation for integrin outside-in signaling. *Blood*. 110:2475–2483. http://dx.doi.org/10.1182/blood-2007-03-080077